Supplementary Material

Aging Trends and Predictive Value of Equivalent Circuit Parameters: The Role of Operating Conditions in Battery State-of-Health Estimation

Mücahit Kutal and Birol Arifoğlu
Manuscript ID: batteries-4598887

This supplement presents additional analyses of the primary population of 12,643 measurements from 30 cells. Absolute SOH errors are in percentage points (pp); MAPE is a relative percentage. Supplementary tables and figures have their own S-prefixed numbering. T_{age} denotes the main article's T_{cha}. Supplementary Software S1 contains machine-readable versions, exact settings, held-out predictions, and code. Supplementary Methods, Section S1, documents the software environment, input precision, model-selection settings, and explicit use of the code module. The code and processed data are provided as supplementary files accompanying the article.

Contents. Tables S1–S14: cell/fold coverage; all 44 scenarios; fold metrics; interventional gain/SHAP; XGBoost settings; paired intervals; dynamic cells; parameter distributions; bootstrap widths; GPR/Ridge settings; path-dependent SHAP; SOH strata; measurement noise; permutation sensitivity. Figures S1–S7 show the trajectory of checkup medians for every cell; Figures S8–S10 show representative fits, bound sensitivity, and resistance–temperature dependence. Tables S15–S19 give all-cell trend summaries, bound counts, sensitivity/transfer results, runtimes, and additional interventional SHAP summaries. Figures S11–S15 report preprocessing, fit quality, parity, interventional SHAP, and correlations. Figure S16 and Table S20 give cell-specific time-constant distributions and bound counts. Supplementary Methods S1 documents the software and reproducibility settings.

Table S1: Cell and fold inventory.

Cell	Fold	T_{age}	SOC (%)	Aging	Checkups	n	SOH (%)
C01B02	4	25	0–100	CC	5	158	78.76–101.44
C02B02	3	25	0–100	CC	5	154	78.20–101.56
C03B02	2	25	0–100	CC	5	154	78.40–101.56
C03B03	5	23	35–65	CC	8	309	82.48–99.00
C04B02	5	25	0–100	CC	5	152	78.60–101.28
C04B03	1	23	35–65	CC	9	353	86.48–99.28
C05B02	5	25	20–50	CC	16	536	79.92–101.36
C05B03	3	23	15–85	CC	7	218	69.28–100.24
C06B02	4	25	20–50	CC	16	532	75.44–101.68
C06B03	4	23	15–85	CC	7	236	77.36–99.52
C07B02	1	25	20–50	CC	6	203	91.04–101.28
C08B02	2	25	20–50	CC	16	528	75.92–101.64
C09B02	5	25	50–80	CC	16	565	80.44–100.72
C10B02	1	25	50–80	CC	16	575	80.20–100.52
C11B02	4	25	50–80	CC	17	596	79.52–99.64
C12B02	3	25	50–80	CC	16	566	79.84–100.48
C13B02	5	45	50–80	CC	13	488	79.12–101.64
C14B02	2	45	50–80	CC	13	479	79.72–101.60
C15B02	2	45	50–80	CC	13	494	78.96–101.56
C16B02	4	45	50–80	CC	13	485	79.44–101.48
C17B02	3	45	20–50	CC	14	525	79.72–101.76
C18B02	3	45	20–50	CC	15	559	79.12–101.52
C19B02	2	45	20–50	CC	15	560	79.20–101.68
C20B02	1	45	20–50	CC	15	563	78.92–101.84
C21B02	4	45	0–100	CC	14	516	76.96–101.28
C22B02	3	45	0–100	CC	14	510	77.96–100.96
C23B02	5	45	0–100	CC	13	477	77.04–101.36
C24B02	1	45	0–100	CC	14	508	77.00–101.40
C25B02	1	23	0–100	Dynamic	8	326	85.56–99.84
C26B02	2	23	0–100	Dynamic	8	318	84.84–99.76

Cell codes retain both the C and B identifiers, since the C number alone is not unique. Temperature is in degrees Celsius. CC denotes constant-current aging; dynamic denotes the source protocol. Checkup counts refer to files with fitted segments.

Table S2: All 44 model scenarios and pooled held-out metrics.

Experiment	n	MAPE	MAE	RMSE	R^2	MaxAE
Ref. XGBoost_M1	12643	2.0136	1.777	2.464	0.8502	20.243
Ref. XGBoost_M2	12643	1.4444	1.275	1.674	0.9309	8.018
Ref. XGBoost_M3	12643	1.6884	1.492	2.261	0.8739	17.751
Ref. XGBoost_M4	12643	1.0235	0.905	1.231	0.9626	8.785
Comp. XGBoost_M0	12643	5.1115	4.523	5.841	0.1582	19.927
Comp. XGBoost_M2A	12643	1.6313	1.443	1.839	0.9166	9.200
Comp. XGBoost_M2B	12643	1.4691	1.300	1.709	0.9279	10.617
Comp. Ridge_M0	12643	5.3630	4.780	6.002	0.1113	19.766
Comp. Ridge_M1	12643	4.7901	4.230	5.176	0.3390	17.561
Comp. Ridge_M2	12643	3.4906	3.090	4.010	0.6034	24.332
Comp. Ridge_M3	12643	4.6790	4.131	5.133	0.3499	17.042
Comp. Ridge_M4	12643	3.2377	2.873	3.758	0.6515	23.176
Comp. Ridge_M2A	12643	3.5637	3.152	4.067	0.5919	26.004
Comp. Ridge_M2B	12643	3.4925	3.089	4.004	0.6044	24.973
Comp. GPR_M0	12643	5.0503	4.461	5.996	0.1130	22.168
Comp. GPR_M1	12643	2.2942	2.033	2.773	0.8103	17.124
Comp. GPR_M2	12643	1.6126	1.425	1.824	0.9179	9.658
Comp. GPR_M3	12643	2.4409	2.171	3.162	0.7534	16.890
Comp. GPR_M4	12643	1.1209	0.998	1.373	0.9535	9.566
ablation_XGBoost_M1_no_R0	12643	2.2198	1.969	2.680	0.8228	19.568
ablation_XGBoost_M1_no_R_DCIR	12643	2.1635	1.911	2.618	0.8308	19.219
ablation_XGBoost_M4_no_R0	12643	1.1917	1.058	1.436	0.9492	9.029
ablation_XGBoost_M4_no_R_DCIR	12643	1.0597	0.937	1.269	0.9603	8.563
ablation_Ridge_M1_no_R0	12643	4.9410	4.375	5.350	0.2937	21.532
ablation_Ridge_M1_no_R_DCIR	12643	4.8198	4.258	5.198	0.3333	17.226
ablation_Ridge_M4_no_R0	12643	3.4110	3.038	3.982	0.6088	29.316
ablation_Ridge_M4_no_R_DCIR	12643	3.2344	2.870	3.758	0.6516	23.243
ablation_GPR_M1_no_R0	12643	2.3978	2.129	2.884	0.7947	16.157
ablation_GPR_M1_no_R_DCIR	12643	2.3422	2.075	2.821	0.8037	16.619
ablation_GPR_M4_no_R0	12643	1.2448	1.111	1.543	0.9412	32.970
ablation_GPR_M4_no_R_DCIR	12643	1.1400	1.015	1.392	0.9522	12.579
No_Bounds_XGBoost_M1	9398	2.1358	1.882	2.601	0.8310	19.568
No_Bounds_XGBoost_M4	9398	1.0754	0.949	1.284	0.9588	8.933
Quality_XGBoost_M1	12596	2.0114	1.776	2.461	0.8511	19.668
Quality_XGBoost_M4	12596	1.0337	0.914	1.246	0.9618	8.779
Wide_Bounds_XGBoost_M1	12643	2.0531	1.812	2.515	0.8439	20.404
Wide_Bounds_XGBoost_M4	12643	1.0498	0.928	1.260	0.9608	8.172
Leave_Temperature_Out_XGBoost_M1	12643	7.6768	6.635	8.681	-0.8593	22.543
Leave_Temperature_Out_XGBoost_M4	12643	6.7007	5.776	7.788	-0.4963	22.225
Leave_SOC_Window_Out_XGBoost_M1	12643	2.6111	2.299	2.946	0.7859	18.330
Leave_SOC_Window_Out_XGBoost_M4	12643	2.6976	2.373	2.833	0.8020	13.713
CC_to_Dynamic_XGBoost_M4	644	3.1904	2.838	3.413	0.4406	8.549
CC_to_Dynamic_Ridge_M4	644	3.5432	3.201	4.170	0.1648	16.640
CC_to_Dynamic_GPR_M4	644	4.6805	4.166	5.829	-0.6318	43.651

MAPE is in percent; MAE, RMSE, and MaxAE are in SOH percentage points. Experiment names are exact Software S1 identifiers; R_DCIR means the pulse-to-rest indicator, not a pure polarization resistance.

Table S3: Original XGBoost metrics in each held-out fold.

Inputs	Fold	MAPE (%)	MAE (pp)	RMSE (pp)	R^2
M1	1	1.9361	1.725	2.380	0.8478
M1	2	1.9886	1.778	2.478	0.8494
M1	3	1.9651	1.711	2.480	0.8590
M1	4	2.0921	1.831	2.418	0.8583
M1	5	2.0865	1.842	2.559	0.8285
M2	1	1.3320	1.196	1.605	0.9308
M2	2	1.4008	1.250	1.602	0.9371
M2	3	1.6017	1.403	1.842	0.9222
M2	4	1.3995	1.220	1.582	0.9394
M2	5	1.4877	1.306	1.723	0.9223
M3	1	1.5857	1.417	2.147	0.8762
M3	2	1.9123	1.698	2.533	0.8426
M3	3	1.7138	1.493	2.292	0.8796
M3	4	1.5233	1.341	2.044	0.8988
M3	5	1.7062	1.510	2.258	0.8664
M4	1	1.1276	1.009	1.350	0.9510
M4	2	1.0188	0.903	1.206	0.9643
M4	3	0.9455	0.833	1.174	0.9684
M4	4	0.9146	0.803	1.050	0.9733
M4	5	1.1110	0.980	1.350	0.9523

Table S4: Fold-specific XGBoost gain and held-out interventional Tree-SHAP values.

Inputs	Fold	Feature	Gain (%)	SHAP (pp)	SHAP (%)
M1	1	R_0	26.780	4.2028	42.162
M1	1	R_1	5.154	0.5002	5.018
M1	1	R_2	7.296	0.6693	6.714
M1	1	R_{pr}	29.524	2.2337	22.409
M1	1	τ_1	3.832	0.4255	4.269
M1	1	τ_2	5.652	0.4871	4.886
M1	1	V_∞	21.761	1.4496	14.543
M1	2	R_0	29.894	3.9812	45.532
M1	2	R_1	5.620	0.5117	5.852
M1	2	R_2	6.750	0.6707	7.670
M1	2	R_{pr}	26.596	1.4595	16.692
M1	2	τ_1	3.799	0.3492	3.993
M1	2	τ_2	5.481	0.4611	5.273
M1	2	V_∞	21.861	1.3105	14.988
M1	3	R_0	27.729	3.8231	42.541
M1	3	R_1	5.311	0.3878	4.315
M1	3	R_2	7.014	0.9408	10.469
M1	3	R_{pr}	29.032	1.5012	16.705
M1	3	τ_1	3.553	0.3587	3.992
M1	3	τ_2	5.342	0.5911	6.578
M1	3	V_∞	22.020	1.3840	15.400
M1	4	R_0	27.225	3.7491	40.504
M1	4	R_1	6.556	0.5496	5.938
M1	4	R_2	7.688	0.8312	8.980
M1	4	R_{pr}	25.843	1.5831	17.103
M1	4	τ_1	4.595	0.4103	4.433
M1	4	τ_2	6.767	0.7511	8.115
M1	4	V_∞	21.326	1.3817	14.927
M1	5	R_0	29.506	4.1912	43.073
M1	5	R_1	6.515	0.5175	5.319
M1	5	R_2	8.121	0.7645	7.857
M1	5	R_{pr}	26.339	1.6373	16.826
M1	5	τ_1	4.135	0.4907	5.043
M1	5	τ_2	6.428	0.8146	8.371
M1	5	V_∞	18.956	1.3146	13.510
M2	1	R_0	24.359	3.2786	25.584
M2	1	R_1	1.420	0.3990	3.113
M2	1	R_2	1.510	0.2504	1.954
M2	1	R_{pr}	14.792	1.6308	12.725
M2	1	τ_1	0.627	0.2273	1.774
M2	1	τ_2	0.637	0.1245	0.971
M2	1	V_∞	7.568	1.4439	11.267
M2	1	T_{age}	23.539	0.8317	6.490
M2	1	T_{beg}	15.424	2.3110	18.034
M2	1	T_{end}	10.123	2.3180	18.088
M2	2	R_0	31.155	4.2024	33.104
M2	2	R_1	1.125	0.2792	2.199
M2	2	R_2	1.860	0.2561	2.017
M2	2	R_{pr}	7.467	1.2532	9.872
M2	2	τ_1	0.723	0.1671	1.316
M2	2	τ_2	0.672	0.1293	1.019
M2	2	V_∞	7.615	1.3868	10.925
M2	2	T_{age}	18.424	0.7199	5.671
M2	2	T_{beg}	12.734	2.0676	16.287
M2	2	T_{end}	18.225	2.2331	17.591
M2	3	R_0	24.695	4.2411	29.401
M2	3	R_1	0.644	0.4855	3.366
M2	3	R_2	0.651	0.2897	2.009
M2	3	R_{pr}	9.376	1.3966	9.681
M2	3	τ_1	0.471	0.2721	1.887
M2	3	τ_2	0.449	0.1672	1.159
M2	3	V_∞	6.292	1.7761	12.313
M2	3	T_{age}	29.021	1.0285	7.130

Inputs	Fold	Feature	Gain (%)	SHAP (pp)	SHAP (%)
M2	3	T_{beg}	11.115	2.2180	15.376
M2	3	T_{end}	17.285	2.5503	17.679
M2	4	R_0	23.264	3.8889	29.246
M2	4	R_1	0.735	0.4531	3.407
M2	4	R_2	0.858	0.2494	1.876
M2	4	R_{pr}	5.036	1.5238	11.460
M2	4	τ_1	0.572	0.2742	2.062
M2	4	τ_2	0.651	0.1893	1.424
M2	4	V_∞	6.986	1.6066	12.083
M2	4	T_{age}	40.315	0.9692	7.289
M2	4	T_{beg}	8.946	1.9760	14.861
M2	4	T_{end}	12.637	2.1664	16.292
M2	5	R_0	25.085	3.9961	30.686
M2	5	R_1	0.651	0.3996	3.068
M2	5	R_2	0.820	0.3127	2.401
M2	5	R_{pr}	6.798	1.4118	10.841
M2	5	τ_1	0.333	0.2503	1.922
M2	5	τ_2	0.416	0.1298	0.997
M2	5	V_∞	6.514	1.5576	11.961
M2	5	T_{age}	36.790	0.7233	5.554
M2	5	T_{beg}	15.586	2.2645	17.389
M2	5	T_{end}	7.009	1.9769	15.181
M3	1	R_0	24.322	4.3647	37.643
M3	1	R_1	4.108	0.4447	3.835
M3	1	R_2	5.392	0.8821	7.608
M3	1	R_{pr}	21.832	2.2124	19.081
M3	1	τ_1	2.990	0.4643	4.005
M3	1	τ_2	3.789	0.7848	6.769
M3	1	V_∞	16.497	1.5607	13.461
M3	1	s_{min}	8.482	0.4343	3.746
M3	1	s_{max}	12.589	0.4468	3.854
M3	2	R_0	27.945	5.0989	43.763
M3	2	R_1	3.204	0.4183	3.590
M3	2	R_2	4.275	0.8675	7.446
M3	2	R_{pr}	17.227	1.7566	15.076
M3	2	τ_1	1.998	0.4921	4.224
M3	2	τ_2	2.601	0.6017	5.165
M3	2	V_∞	14.782	1.4954	12.835
M3	2	s_{min}	18.177	0.5716	4.906
M3	2	s_{max}	9.791	0.3491	2.997
M3	3	R_0	25.462	4.8537	37.483
M3	3	R_1	3.986	0.4395	3.394
M3	3	R_2	5.531	1.4108	10.895
M3	3	R_{pr}	15.233	1.9620	15.151
M3	3	τ_1	1.951	0.5373	4.149
M3	3	τ_2	2.934	0.9195	7.101
M3	3	V_∞	14.201	1.8187	14.045
M3	3	s_{min}	7.548	0.3500	2.703
M3	3	s_{max}	23.155	0.6578	5.080
M3	4	R_0	29.552	5.4970	37.219
M3	4	R_1	4.741	0.6703	4.539
M3	4	R_2	6.261	1.4017	9.491
M3	4	R_{pr}	19.305	2.2643	15.331
M3	4	τ_1	2.980	0.6117	4.141
M3	4	τ_2	4.025	1.1933	8.080
M3	4	V_∞	15.123	2.0321	13.759
M3	4	s_{min}	9.020	0.5164	3.496
M3	4	s_{max}	8.993	0.5824	3.943
M3	5	R_0	29.707	4.2970	38.688
M3	5	R_1	4.054	0.4911	4.421
M3	5	R_2	4.904	0.8458	7.615
M3	5	R_{pr}	19.559	1.7174	15.462
M3	5	τ_1	2.292	0.4853	4.370
M3	5	τ_2	3.652	0.8522	7.673
M3	5	V_∞	16.230	1.4231	12.813
M3	5	s_{min}	6.751	0.3079	2.773

Inputs	Fold	Feature	Gain (%)	SHAP (pp)	SHAP (%)
M3	5	$s_{\max}$	12.851	0.6871	6.186
M4	1	R_0	24.768	4.1302	28.583
M4	1	R_1	0.505	0.4392	3.040
M4	1	R_2	0.461	0.0720	0.498
M4	1	R_{pr}	6.769	0.9929	6.871
M4	1	τ_1	0.291	0.3333	2.307
M4	1	τ_2	0.207	0.0914	0.633
M4	1	V_∞	6.280	1.4325	9.914
M4	1	T_{age}	18.882	1.1395	7.886
M4	1	T_{beg}	19.080	2.6628	18.428
M4	1	T_{end}	11.314	2.0946	14.496
M4	1	$s_{\min}$	6.459	0.5233	3.622
M4	1	$s_{\max}$	4.985	0.5379	3.722
M4	2	R_0	25.953	4.7093	32.589
M4	2	R_1	0.771	0.3158	2.185
M4	2	R_2	1.157	0.1298	0.899
M4	2	R_{pr}	4.701	1.1396	7.886
M4	2	τ_1	0.327	0.3161	2.187
M4	2	τ_2	0.312	0.0726	0.502
M4	2	V_∞	6.241	1.6576	11.471
M4	2	T_{age}	21.357	1.2992	8.990
M4	2	T_{beg}	9.557	1.8800	13.010
M4	2	T_{end}	16.139	1.8392	12.728
M4	2	$s_{\min}$	7.501	0.6016	4.164
M4	2	$s_{\max}$	5.984	0.4896	3.388
M4	3	R_0	21.434	4.0526	31.028
M4	3	R_1	0.408	0.2346	1.796
M4	3	R_2	0.542	0.0851	0.652
M4	3	R_{pr}	5.498	0.8908	6.821
M4	3	τ_1	0.332	0.1915	1.466
M4	3	τ_2	0.291	0.0646	0.495
M4	3	V_∞	6.926	1.5249	11.676
M4	3	T_{age}	24.627	0.6222	4.764
M4	3	T_{beg}	12.703	1.9807	15.165
M4	3	T_{end}	16.855	2.1893	16.762
M4	3	$s_{\min}$	5.556	0.6682	5.116
M4	3	$s_{\max}$	4.828	0.5564	4.260
M4	4	R_0	21.248	4.3329	31.266
M4	4	R_1	0.490	0.3068	2.214
M4	4	R_2	0.619	0.1107	0.799
M4	4	R_{pr}	8.915	1.2103	8.734
M4	4	τ_1	0.257	0.2636	1.902
M4	4	τ_2	0.244	0.0732	0.528
M4	4	V_∞	7.338	1.6198	11.689
M4	4	T_{age}	23.483	0.9602	6.929
M4	4	T_{beg}	13.515	2.0275	14.631
M4	4	T_{end}	13.451	1.9161	13.827
M4	4	$s_{\min}$	5.541	0.5414	3.907
M4	4	$s_{\max}$	4.898	0.4953	3.574
M4	5	R_0	20.186	4.4274	31.975
M4	5	R_1	0.450	0.3420	2.470
M4	5	R_2	0.408	0.0934	0.674
M4	5	R_{pr}	5.058	1.2127	8.758
M4	5	τ_1	0.230	0.3179	2.296
M4	5	τ_2	0.217	0.0784	0.566
M4	5	V_∞	5.543	1.6177	11.683
M4	5	T_{age}	34.891	1.0050	7.258
M4	5	T_{beg}	10.252	1.9133	13.818
M4	5	T_{end}	9.402	1.8750	13.542
M4	5	$s_{\min}$	4.998	0.3155	2.279
M4	5	$s_{\max}$	8.364	0.6480	4.680

Gain and relative SHAP are normalized separately within each model and fold. The absolute SHAP column uses the SOH output scale. These explanations use the common interventional convention; Table S11 retains the original path-dependent explanations.

Table S5: Selected outer-fold XGBoost hyperparameters for the original four configurations.

Inputs	Fold	Trees	Depth	Rate	Subsample	Columns	λ
M1	1	1000	9	0.016811	0.664494	0.888691	0.272314
M1	2	1250	10	0.021902	0.665126	0.931073	8.472906
M1	3	1150	10	0.017896	0.841760	0.999982	7.319892
M1	4	1350	10	0.013630	0.552851	0.954741	3.546136
M1	5	850	8	0.024246	0.550967	0.964593	2.699050
M2	1	1050	5	0.064121	0.746502	0.770469	5.962952
M2	2	1300	6	0.030456	0.871845	0.696818	3.408008
M2	3	1400	4	0.066728	0.770796	0.940115	2.929194
M2	4	1300	5	0.089274	0.579693	0.812454	3.831679
M2	5	1500	5	0.052494	0.943874	0.898444	5.371885
M3	1	1050	8	0.029333	0.531022	0.970866	2.393863
M3	2	900	8	0.092993	0.677251	0.963912	8.479713
M3	3	1000	7	0.048803	0.737760	0.944046	6.539834
M3	4	1300	6	0.040880	0.610722	0.902486	4.319257
M3	5	1450	8	0.028510	0.661137	0.999598	8.294266
M4	1	850	4	0.087154	0.775506	0.949527	0.213459
M4	2	1350	5	0.049894	0.707804	0.564196	0.150025
M4	3	1100	7	0.029051	0.509547	0.952301	6.563050
M4	4	750	5	0.085140	0.768186	0.771461	0.252279
M4	5	1450	5	0.100799	0.605578	0.803460	0.633040

All selected settings for all models and scenarios are included as JSON files in Software S1; additional GPR and Ridge settings are summarized in Table S10.

Table S6: Paired cell-bootstrap differences in MAPE (A minus B).

A	B	Common n	Difference	95% interval
XGB M1	XGB M0	12643	-2.8105	[-3.4930, -2.1532]
XGB M1	XGB M2	12643	0.6265	[0.4876, 0.7689]
XGB M1	XGB M3	12643	0.2838	[0.0850, 0.4843]
XGB M1	XGB M4	12643	1.0687	[0.8608, 1.2862]
XGB M1_no_R0	XGB M1	12643	0.2181	[0.1500, 0.2834]
XGB M1_no_R_DCIR	XGB M1	12643	0.1665	[0.1179, 0.2189]
XGB M4_no_R0	XGB M4	12643	0.1593	[0.1057, 0.2173]
XGB M4_no_R_DCIR	XGB M4	12643	0.0347	[0.0143, 0.0556]
Ridge_M1	Ridge_M0	12643	-0.5908	[-1.0316, -0.1189]
Ridge_M1	Ridge_M2	12643	1.3653	[1.0999, 1.6591]
Ridge_M1	Ridge_M3	12643	0.0933	[-0.2650, 0.4343]
Ridge_M1	Ridge_M4	12643	1.6044	[1.2895, 1.9557]
Ridge_M1_no_R0	Ridge_M1	12643	0.1634	[0.1009, 0.2378]
Ridge_M1_no_R_DCIR	Ridge_M1	12643	0.0279	[0.0037, 0.0573]
Ridge_M4_no_R0	Ridge_M4	12643	0.1507	[0.0639, 0.2311]
Ridge_M4_no_R_DCIR	Ridge_M4	12643	-0.0042	[-0.0089, 0.0001]
GPR_M1	GPR_M0	12643	-2.2948	[-3.1658, -1.4582]
GPR_M1	GPR_M2	12643	0.7269	[0.5718, 0.8839]
GPR_M1	GPR_M3	12643	-0.2242	[-0.4525, 0.0341]
GPR_M1	GPR_M4	12643	1.2224	[0.9813, 1.4698]
GPR_M1_no_R0	GPR_M1	12643	0.1398	[0.0744, 0.2080]
GPR_M1_no_R_DCIR	GPR_M1	12643	0.0866	[0.0349, 0.1478]
GPR_M4_no_R0	GPR_M4	12643	0.1448	[0.1007, 0.1973]
GPR_M4_no_R_DCIR	GPR_M4	12643	0.0232	[0.0106, 0.0373]
XGB M0	GPR_M0	12643	0.2340	[-0.0204, 0.5223]
XGB M0	Ridge_M0	12643	-0.5068	[-1.0426, 0.0745]
XGB M1	GPR_M1	12643	-0.2817	[-0.3694, -0.1858]
XGB M1	Ridge_M1	12643	-2.7264	[-3.0812, -2.3453]
XGB M2	GPR_M2	12643	-0.1813	[-0.2844, -0.0793]
XGB M2	Ridge_M2	12643	-1.9876	[-2.3041, -1.6489]
XGB M3	GPR_M3	12643	-0.7897	[-0.9342, -0.6488]
XGB M3	Ridge_M3	12643	-2.9169	[-3.2928, -2.5047]
XGB M4	GPR_M4	12643	-0.1280	[-0.1865, -0.0656]
XGB M4	Ridge_M4	12643	-2.1907	[-2.4896, -1.8747]
XGB M1	No_Bounds_XGB M1	9398	-0.0484	[-0.0747, -0.0230]
XGB M4	No_Bounds_XGB M4	9398	-0.0356	[-0.0547, -0.0160]
XGB M1	Quality_XGB M1	12596	-0.0020	[-0.0116, 0.0084]
XGB M4	Quality_XGB M4	12596	-0.0134	[-0.0407, 0.0084]
XGB M1	Wide_Bounds_XGB M1	12643	-0.0438	[-0.0581, -0.0300]
XGB M4	Wide_Bounds_XGB M4	12643	-0.0220	[-0.0557, 0.0001]

Differences average cell-specific MAPE equally over cells. They are not differences of the pooled MAPE values in Table S2. Intervals use 2000 cell resamples, conditional on the fixed fitted predictions. Full MAE, RMSE, and R-squared results are supplied in Software S1.

Table S7: Separate results for the two dynamically aged cells.

Training/test design	Cell	n	MAPE (%)	RMSE (pp)	R^2
Grouped XGBoost	C25B02	326	0.7471	0.866	0.9618
Grouped XGBoost	C26B02	318	1.0622	1.249	0.9292
Grouped GPR	C25B02	326	0.9602	1.197	0.9269
Grouped GPR	C26B02	318	1.3172	1.537	0.8929
Grouped Ridge	C25B02	326	2.7799	3.393	0.4127
Grouped Ridge	C26B02	318	3.3128	3.949	0.2923
CC to dynamic XGBoost	C25B02	326	2.8739	3.138	0.4977
CC to dynamic XGBoost	C26B02	318	3.5149	3.673	0.3878
CC to dynamic GPR	C25B02	326	4.4343	5.569	-0.5819
CC to dynamic GPR	C26B02	318	4.9329	6.083	-0.6792
CC to dynamic Ridge	C25B02	326	3.1956	3.765	0.2770
CC to dynamic Ridge	C26B02	318	3.8995	4.548	0.0615

Grouped results use the original cell folds, where the other dynamic cell may be in training. CC-to-dynamic models are trained only on 28 CC-aged cells. Measurements remain laboratory reference-test measurements in both cases.

Table S8: Distributions in the primary population.

Quantity	Median	5th percentile	95th percentile	Minimum	Maximum
R_0	29.2590	22.3200	43.6300	19.8260	70.4060
R_1	5.4140	2.3311	10.6532	0.0000	31.1570
R_2	13.3650	4.9763	40.9469	1.4770	91.0680
R_{pr}	40.6700	29.7600	58.5460	23.4700	82.7970
τ_1	17.4361	10.0000	28.7488	10.0000	40.0000
τ_2	112.3609	60.8918	200.0000	40.0000	200.0000
V_∞	3.7280	3.5110	4.1367	3.2545	4.1697
fit_rmse_v	0.3871	0.3094	0.5230	0.2372	0.9721
fit_r2	0.9961	0.9845	0.9986	0.9268	0.9995
transition_gap_s	10.0000	10.0000	10.0000	0.1000	10.0000
sampling_median_s	10.0000	10.0000	10.0000	0.1000	10.0000

Resistances are in milliohms; fit RMSE is in millivolts; time constants are in seconds; asymptotic voltage is in volts; fit R-squared is dimensionless.

Table S9: Approximate constrained residual-bootstrap interval widths for 353 representative segments.

Quantity	Segments	Median 95% interval width	Unit
R_1	353	2.373	mΩ
R_2	353	5.205	mΩ
τ_1	353	7.877	s
τ_2	353	83.029	s
V_∞	353	1.949	mV

Each segment uses 50 circular block-residual refits with a block length of 6 samples. These intervals are conditional on the two-exponential model and the selected bounds; they do not establish globally unique electrochemical parameters. Segment-level intervals are in Software S1.

Table S10: Additional-model settings by outer fold.

Model	Inputs	Fold	Selected setting
GPR	M0	1	0.797**2 * Matern(length_scale=0.105, nu=1.5) + WhiteKernel(noise_level=0.585)
GPR	M0	2	0.889**2 * Matern(length_scale=0.13, nu=1.5) + WhiteKernel(noise_level=0.535)
GPR	M0	3	0.868**2 * Matern(length_scale=0.125, nu=1.5) + WhiteKernel(noise_level=0.573)
GPR	M0	4	0.804**2 * Matern(length_scale=0.111, nu=1.5) + WhiteKernel(noise_level=0.539)
GPR	M0	5	0.792**2 * Matern(length_scale=0.123, nu=1.5) + WhiteKernel(noise_level=0.617)
GPR	M1	1	1.2**2 * Matern(length_scale=1.67, nu=1.5) + WhiteKernel(noise_level=0.206)
GPR	M1	2	1.43**2 * Matern(length_scale=2.3, nu=1.5) + WhiteKernel(noise_level=0.222)
GPR	M1	3	1.35**2 * Matern(length_scale=1.87, nu=1.5) + WhiteKernel(noise_level=0.193)
GPR	M1	4	1.39**2 * Matern(length_scale=2.12, nu=1.5) + WhiteKernel(noise_level=0.245)
GPR	M1	5	1.47**2 * Matern(length_scale=2.29, nu=1.5) + WhiteKernel(noise_level=0.213)
GPR	M2	1	11.6**2 * Matern(length_scale=17.7, nu=1.5) + WhiteKernel(noise_level=0.0631)
GPR	M2	2	8.6**2 * Matern(length_scale=15.4, nu=1.5) + WhiteKernel(noise_level=0.0708)
GPR	M2	3	10.9**2 * Matern(length_scale=18.1, nu=1.5) + WhiteKernel(noise_level=0.0627)
GPR	M2	4	9.88**2 * Matern(length_scale=17.3, nu=1.5) + WhiteKernel(noise_level=0.0679)
GPR	M2	5	7.6**2 * Matern(length_scale=13.9, nu=1.5) + WhiteKernel(noise_level=0.0668)
GPR	M3	1	3.13**2 * Matern(length_scale=7.57, nu=1.5) + WhiteKernel(noise_level=0.338)
GPR	M3	2	2.46**2 * Matern(length_scale=5.46, nu=1.5) + WhiteKernel(noise_level=0.26)
GPR	M3	3	5.12**2 * Matern(length_scale=10.1, nu=1.5) + WhiteKernel(noise_level=0.301)
GPR	M3	4	3.73**2 * Matern(length_scale=8.54, nu=1.5) + WhiteKernel(noise_level=0.344)
GPR	M3	5	5.57**2 * Matern(length_scale=10.8, nu=1.5) + WhiteKernel(noise_level=0.289)
GPR	M4	1	19.1**2 * Matern(length_scale=32.6, nu=1.5) + WhiteKernel(noise_level=0.0257)
GPR	M4	2	21.8**2 * Matern(length_scale=37.4, nu=1.5) + WhiteKernel(noise_level=0.0292)
GPR	M4	3	21.2**2 * Matern(length_scale=35.2, nu=1.5) + WhiteKernel(noise_level=0.0289)
GPR	M4	4	16.6**2 * Matern(length_scale=29.4, nu=1.5) + WhiteKernel(noise_level=0.0261)
GPR	M4	5	20.6**2 * Matern(length_scale=34.1, nu=1.5) + WhiteKernel(noise_level=0.0252)
Ridge	M0	1	alpha = 0.0001
Ridge	M0	2	alpha = 0.1
Ridge	M0	3	alpha = 0.0001
Ridge	M0	4	alpha = 0.0001
Ridge	M0	5	alpha = 0.1
Ridge	M1	1	alpha = 0.0001
Ridge	M1	2	alpha = 10
Ridge	M1	3	alpha = 1
Ridge	M1	4	alpha = 10
Ridge	M1	5	alpha = 10
Ridge	M2	1	alpha = 1
Ridge	M2	2	alpha = 100
Ridge	M2	3	alpha = 10
Ridge	M2	4	alpha = 100

Model	Inputs	Fold	Selected setting
Ridge	M2	5	alpha = 100
Ridge	M3	1	alpha = 1
Ridge	M3	2	alpha = 10
Ridge	M3	3	alpha = 10
Ridge	M3	4	alpha = 100
Ridge	M3	5	alpha = 1
Ridge	M4	1	alpha = 1
Ridge	M4	2	alpha = 10
Ridge	M4	3	alpha = 10
Ridge	M4	4	alpha = 10
Ridge	M4	5	alpha = 100

Kernel expressions act on standardized inputs and normalized targets. Exact floating-point values, training statistics, optimization subsets, and seeds are in the accompanying JSON settings.

Table S11: Original path-dependent XGBoost explanations for M1 and M4.

Inputs	Fold	Feature	SHAP (pp)	SHAP (%)
M1	1	R_0	3.4934	41.921
M1	1	R_1	0.3691	4.430
M1	1	R_2	0.6223	7.467
M1	1	R_{pr}	1.7258	20.710
M1	1	τ_1	0.3525	4.231
M1	1	τ_2	0.4369	5.242
M1	1	V_∞	1.3332	15.999
M1	2	R_0	3.5754	43.570
M1	2	R_1	0.4157	5.066
M1	2	R_2	0.6286	7.660
M1	2	R_{pr}	1.3835	16.859
M1	2	τ_1	0.3237	3.945
M1	2	τ_2	0.5239	6.384
M1	2	V_∞	1.3553	16.516
M1	3	R_0	3.3079	41.317
M1	3	R_1	0.4179	5.220
M1	3	R_2	0.7359	9.192
M1	3	R_{pr}	1.2625	15.769
M1	3	τ_1	0.3290	4.109
M1	3	τ_2	0.5569	6.956
M1	3	V_∞	1.3961	17.438
M1	4	R_0	3.5268	42.941
M1	4	R_1	0.4365	5.315
M1	4	R_2	0.7262	8.842
M1	4	R_{pr}	1.4070	17.131
M1	4	τ_1	0.3361	4.092
M1	4	τ_2	0.5788	7.048
M1	4	V_∞	1.2016	14.631
M1	5	R_0	3.7806	42.602
M1	5	R_1	0.4878	5.497
M1	5	R_2	0.7656	8.627
M1	5	R_{pr}	1.5002	16.905
M1	5	τ_1	0.3961	4.464
M1	5	τ_2	0.6419	7.234
M1	5	V_∞	1.3019	14.671
M4	1	R_0	3.6105	29.084
M4	1	R_1	0.3029	2.440
M4	1	R_2	0.0575	0.463
M4	1	R_{pr}	0.6065	4.886
M4	1	τ_1	0.2448	1.972
M4	1	τ_2	0.0608	0.489
M4	1	V_∞	1.6094	12.965
M4	1	T_{age}	0.7876	6.344
M4	1	T_{beg}	2.3073	18.586
M4	1	T_{end}	1.8434	14.849
M4	1	s_{min}	0.4749	3.826
M4	1	s_{max}	0.5085	4.096
M4	2	R_0	3.7812	32.356
M4	2	R_1	0.2018	1.727
M4	2	R_2	0.1242	1.063
M4	2	R_{pr}	0.8376	7.167
M4	2	τ_1	0.2228	1.906
M4	2	τ_2	0.0580	0.497
M4	2	V_∞	1.6062	13.744
M4	2	T_{age}	0.9300	7.958
M4	2	T_{beg}	1.5065	12.891
M4	2	T_{end}	1.5329	13.117
M4	2	s_{min}	0.4795	4.103
M4	2	s_{max}	0.4057	3.472
M4	3	R_0	3.2374	30.614
M4	3	R_1	0.1738	1.644
M4	3	R_2	0.0762	0.721
M4	3	R_{pr}	0.6038	5.710

Inputs	Fold	Feature	SHAP (pp)	SHAP (%)
M4	3	τ_1	0.1692	1.600
M4	3	τ_2	0.0504	0.477
M4	3	V_∞	1.5928	15.062
M4	3	T_{age}	0.3923	3.710
M4	3	T_{beg}	1.4425	13.641
M4	3	T_{end}	1.7635	16.677
M4	3	s_{min}	0.5545	5.244
M4	3	s_{max}	0.5181	4.900
M4	4	R_0	3.5927	31.390
M4	4	R_1	0.2115	1.848
M4	4	R_2	0.1122	0.980
M4	4	R_{pr}	1.0029	8.763
M4	4	τ_1	0.1973	1.724
M4	4	τ_2	0.0513	0.448
M4	4	V_∞	1.5055	13.154
M4	4	T_{age}	0.7066	6.174
M4	4	T_{beg}	1.5796	13.801
M4	4	T_{end}	1.4685	12.831
M4	4	s_{min}	0.5413	4.730
M4	4	s_{max}	0.4758	4.158
M4	5	R_0	3.6930	31.205
M4	5	R_1	0.2618	2.212
M4	5	R_2	0.1004	0.848
M4	5	R_{pr}	0.9189	7.764
M4	5	τ_1	0.2431	2.054
M4	5	τ_2	0.0694	0.586
M4	5	V_∞	1.5204	12.847
M4	5	T_{age}	0.8092	6.838
M4	5	T_{beg}	1.6513	13.953
M4	5	T_{end}	1.6046	13.558
M4	5	s_{min}	0.3621	3.060
M4	5	s_{max}	0.6006	5.075

All held-out rows are explained. These reproduce the original explanation convention and are not mixed with the interventional values in the revised main-text comparison.

Table S12: M4 errors by reference SOH interval.

Model	SOH	n	MAPE	MAE	RMSE	R^2	MaxAE
XGBoost	<80%	871	1.5470	1.209	1.585	-0.5767	8.785
XGBoost	80-90%	6536	0.9822	0.837	1.155	0.8186	5.423
XGBoost	90-100%	4269	1.0065	0.946	1.241	0.8153	7.670
XGBoost	>=100%	967	0.9057	0.917	1.322	-8.7779	7.700
GPR	<80%	871	1.6339	1.278	1.775	-0.9766	7.712
GPR	80-90%	6536	1.0224	0.872	1.228	0.7951	6.428
GPR	90-100%	4269	1.1056	1.039	1.365	0.7765	9.566
GPR	>=100%	967	1.3926	1.411	1.847	-18.0899	7.186
Ridge	<80%	871	6.2476	4.906	5.532	-18.1949	23.176
Ridge	80-90%	6536	2.9163	2.465	3.101	-0.3071	15.559
Ridge	90-100%	4269	2.4401	2.306	3.027	-0.0997	14.834
Ridge	>=100%	967	6.2198	6.308	7.188	-288.1814	18.777

MAPE is a relative percentage; absolute errors are in SOH percentage points. Interval-specific R-squared can be negative when the target variance is small. Full stratum results for all scenarios and cell-bootstrap intervals are in Software S1.

Table S13: Measurement-noise sensitivity on the same 353 representative segments.

Model	σ_V (mV)	Clean RMSE	Noisy RMSE	Noisy MAPE	Mean shift
XGBoost	0.5	1.763	1.833	1.3752	0.442
XGBoost	1.0	1.763	2.001	1.5316	0.688
XGBoost	2.0	1.763	2.405	1.8766	1.081
Ridge	0.5	5.621	5.622	4.6944	0.327
Ridge	1.0	5.621	5.669	4.7161	0.609
Ridge	2.0	5.621	5.755	4.8321	1.189
GPR	0.5	2.004	2.161	1.7428	0.581
GPR	1.0	2.004	2.458	1.9950	1.030
GPR	2.0	2.004	3.238	2.6620	1.835

Each level includes 5 repeats per segment and current noise with standard deviation 0.5 percent of pulse magnitude. SOH labels are fixed. RMSE and absolute prediction shift are in SOH percentage points; MAPE is a relative percentage. Noise levels are illustrative, not measured instrument uncertainties.

Table S14: M4 marginal and joint-group permutation sensitivity.

Model	Permuted group	Mean RMSE increase (pp)	SD (pp)
XGBoost	ECM_joint	8.241	0.920
XGBoost	OCV	2.127	0.361
XGBoost	R0	6.379	0.649
XGBoost	R1	0.184	0.033
XGBoost	R2	0.077	0.035
XGBoost	R_DCIR	1.032	0.290
XGBoost	SOC_joint	1.008	0.345
XGBoost	SOC_max	0.298	0.098
XGBoost	SOC_min	0.444	0.255
XGBoost	T1	0.092	0.061
XGBoost	T2	0.030	0.019
XGBoost	TEMPERATURES_joint	6.677	0.551
XGBoost	T_beg	2.274	0.271
XGBoost	T_cha	0.886	0.271
XGBoost	T_end	2.243	0.227
GPR	ECM_joint	11.130	1.756
GPR	OCV	2.253	0.574
GPR	R0	11.405	1.656
GPR	R1	1.046	0.265
GPR	R2	1.387	0.308
GPR	R_DCIR	2.138	0.347
GPR	SOC_joint	1.378	0.549
GPR	SOC_max	2.313	0.413
GPR	SOC_min	1.343	0.375
GPR	T1	0.271	0.099
GPR	T2	0.415	0.093
GPR	TEMPERATURES_joint	9.546	0.530
GPR	T_beg	9.064	0.645
GPR	T_cha	4.149	1.130
GPR	T_end	2.629	0.874
Ridge	ECM_joint	5.485	0.800
Ridge	OCV	0.066	0.038
Ridge	R0	6.079	0.940
Ridge	R1	0.120	0.108
Ridge	R2	0.062	0.045
Ridge	R_DCIR	0.022	0.079
Ridge	SOC_joint	0.477	0.145
Ridge	SOC_max	0.507	0.163
Ridge	SOC_min	-0.002	0.003
Ridge	T1	0.069	0.043
Ridge	T2	0.003	0.005
Ridge	TEMPERATURES_joint	3.673	0.475
Ridge	T_beg	1.494	0.860
Ridge	T_cha	1.111	0.918
Ridge	T_end	4.616	4.895

Feature names match the software columns: OCV, R_DCIR, T1, and T2 correspond to V_∞, R_{pr}, τ_1, and τ_2, respectively. Summaries combine five repetitions in each of five held-out folds (up to 40 rows per cell). SD describes these perturbations and is not a cell-bootstrap confidence interval. Joint group members share the same permutation. Correlated-feature perturbations can produce uncommon input combinations and are not causal interventions.

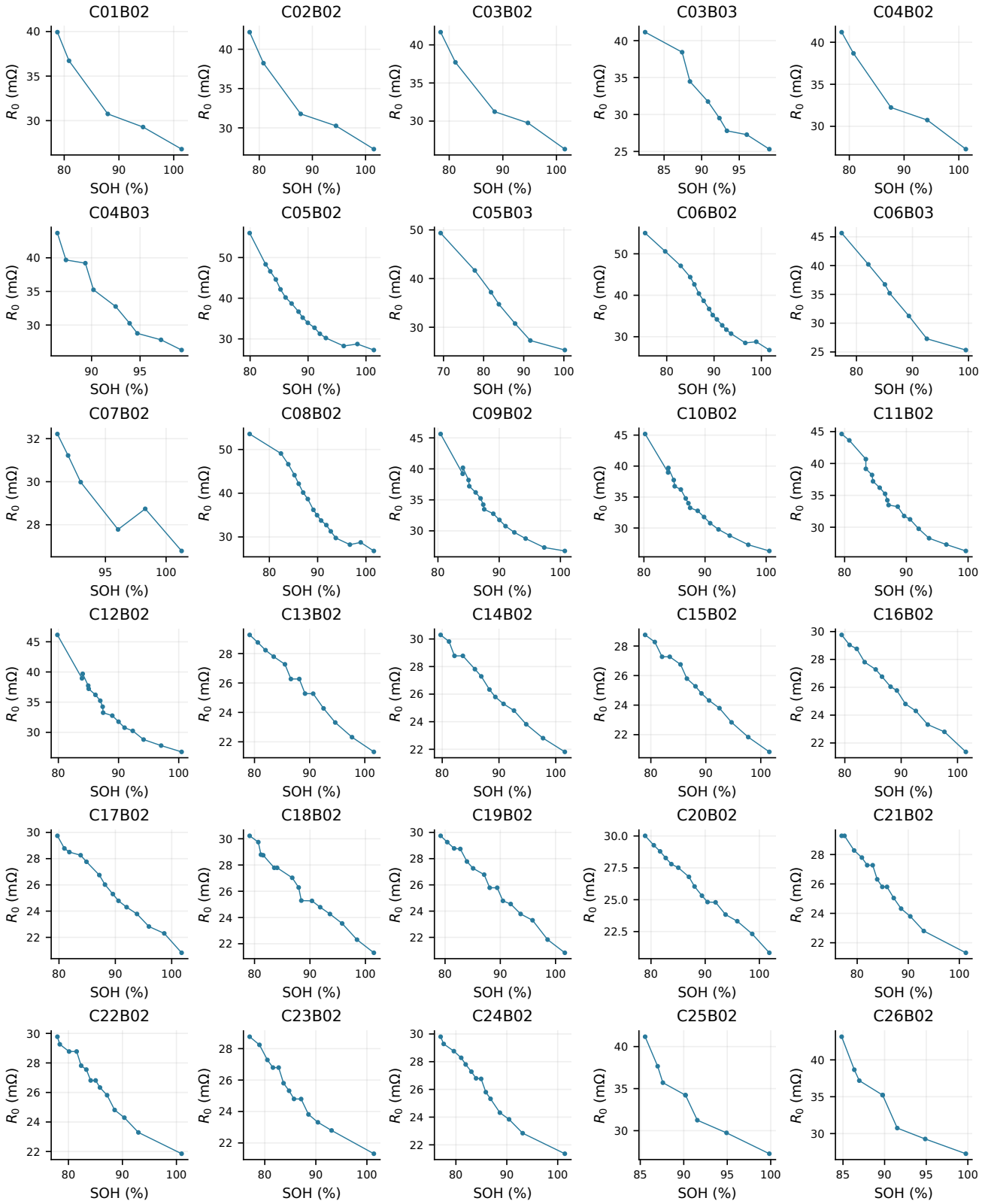


Figure S1: Checkup-median R_0 versus SOH for all 30 cells. Lines join observations; the full C/B cell identifiers are shown. The operating points are not matched in instantaneous SOC or temperature. These are descriptive trajectories, not causal aging estimates.

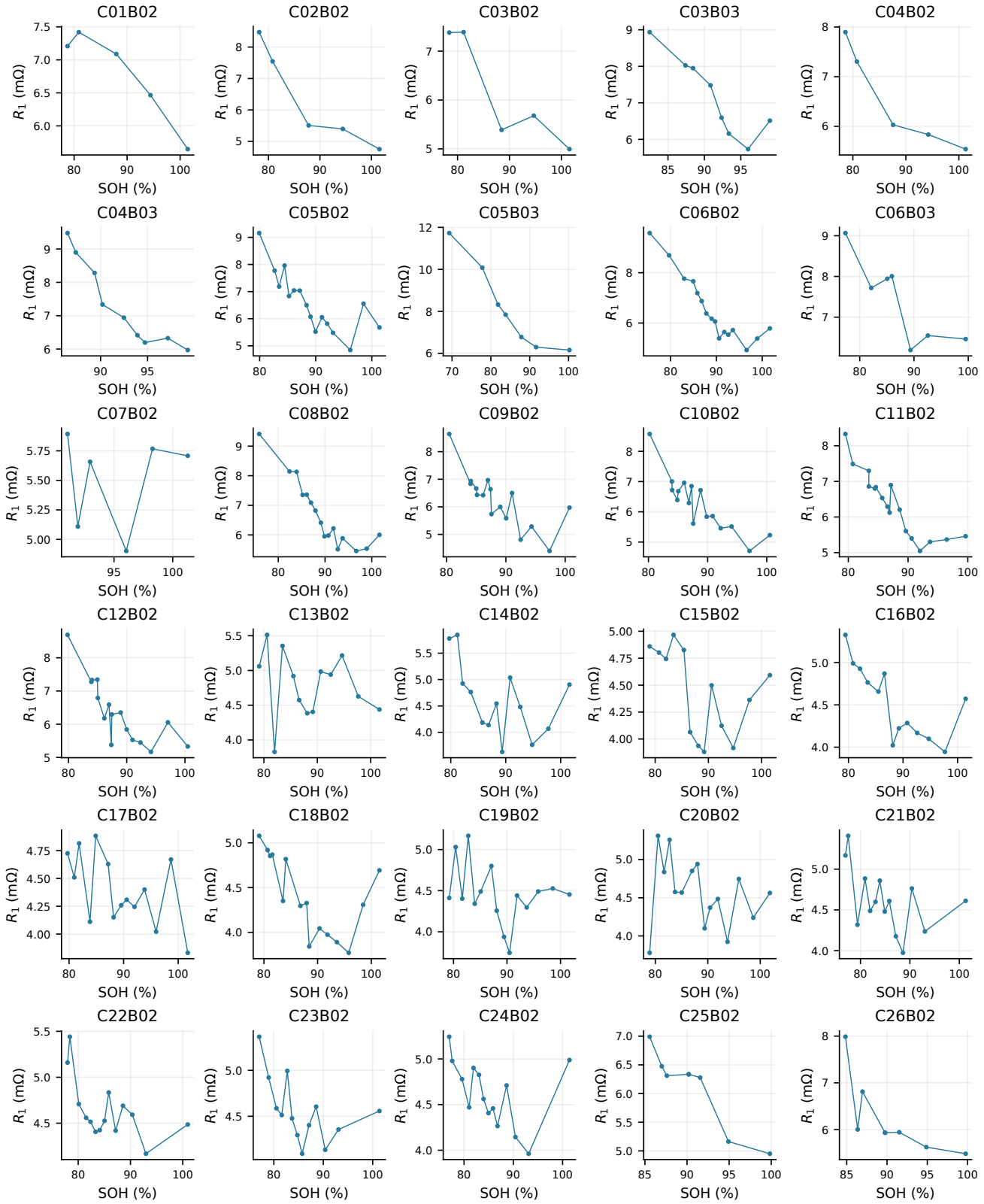


Figure S2: Checkup-median R_1 versus SOH for all 30 cells. Lines join observations; the full C/B cell identifiers are shown. The operating points are not matched in instantaneous SOC or temperature. These are descriptive trajectories, not causal aging estimates.

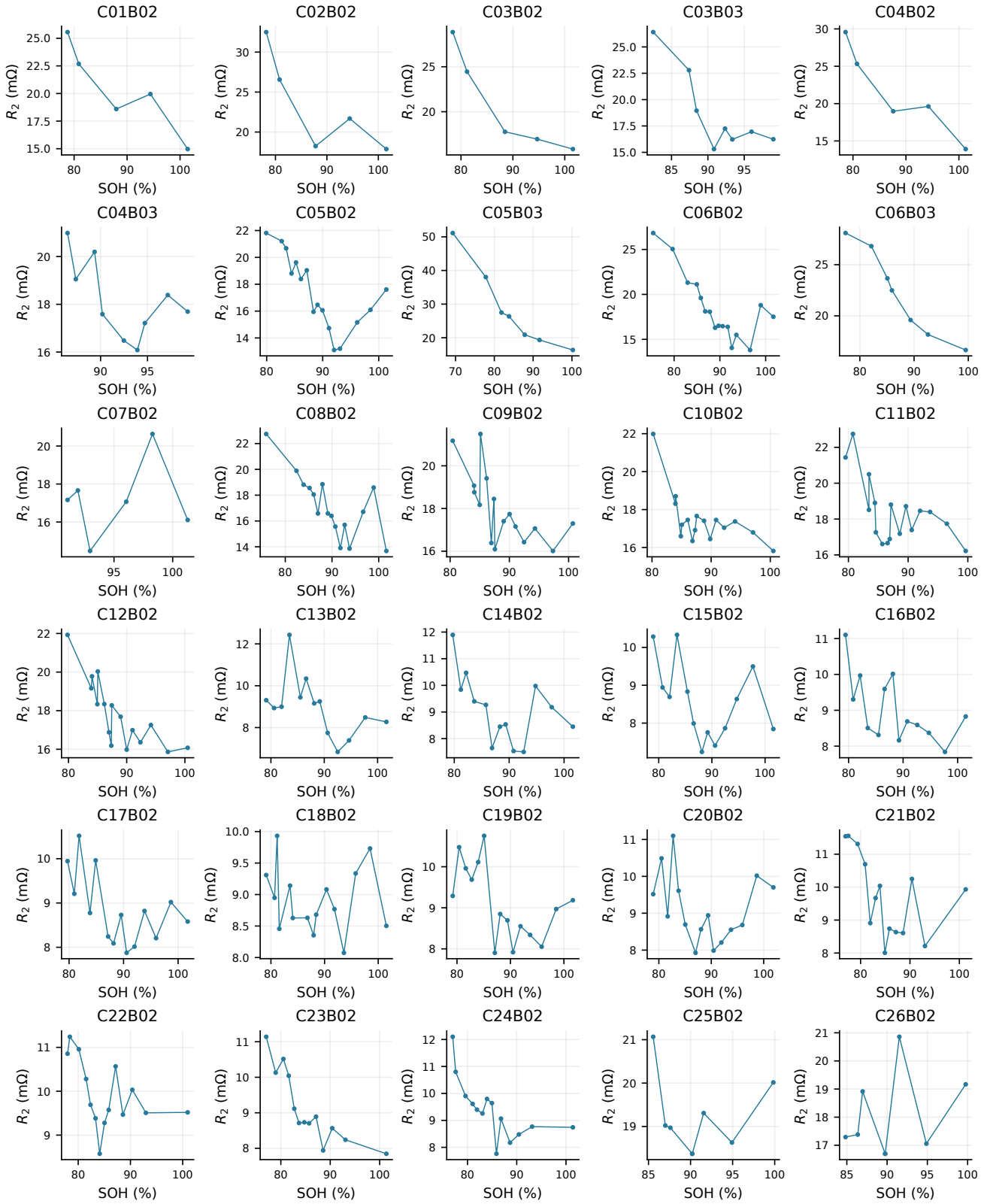


Figure S3: Checkup-median R_2 versus SOH for all 30 cells. Lines join observations; the full C/B cell identifiers are shown. The operating points are not matched in instantaneous SOC or temperature. These are descriptive trajectories, not causal aging estimates.

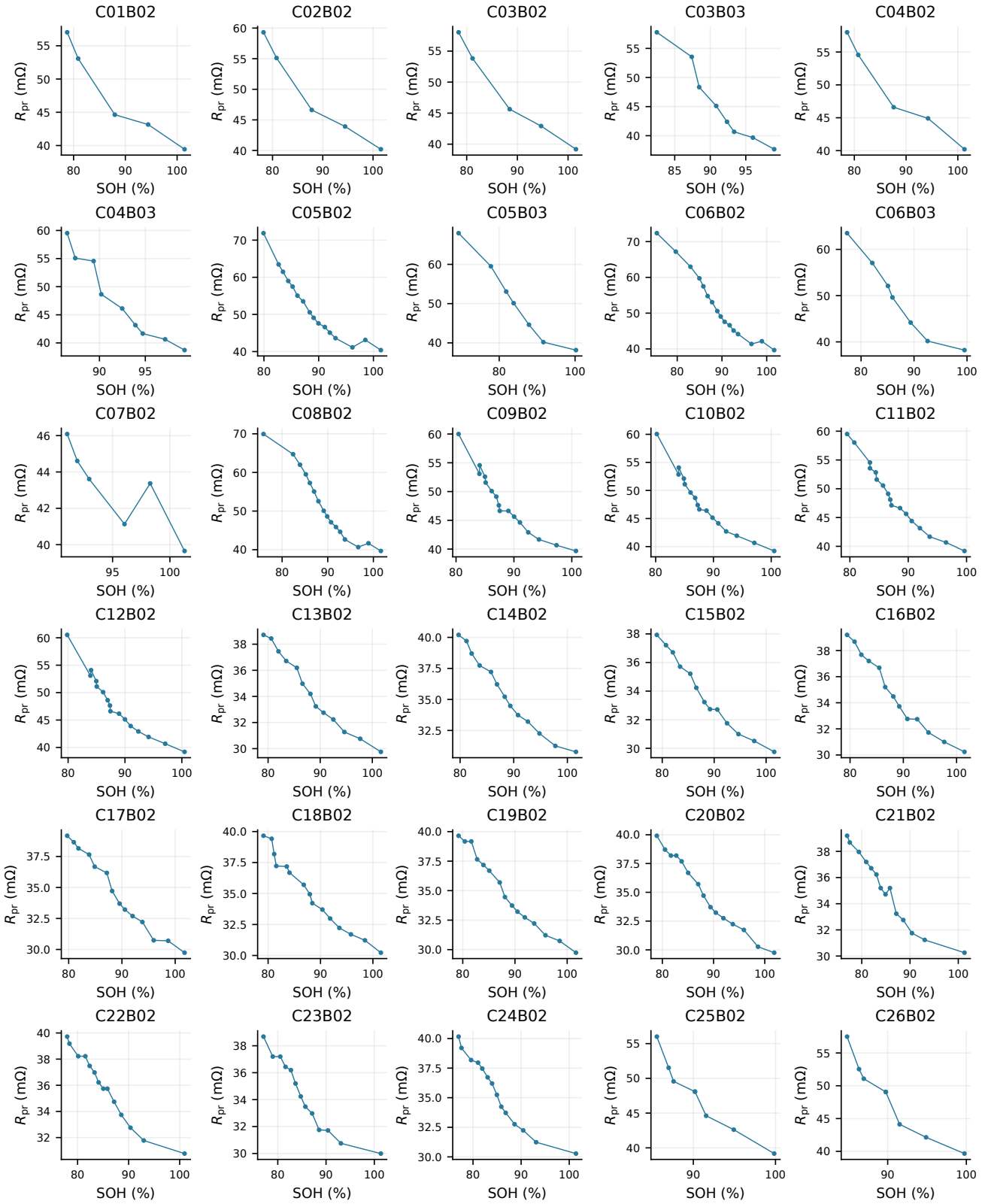


Figure S4: Checkup-median R_{pr} versus SOH for all 30 cells. Lines join observations; the full C/B cell identifiers are shown. The operating points are not matched in instantaneous SOC or temperature. These are descriptive trajectories, not causal aging estimates.

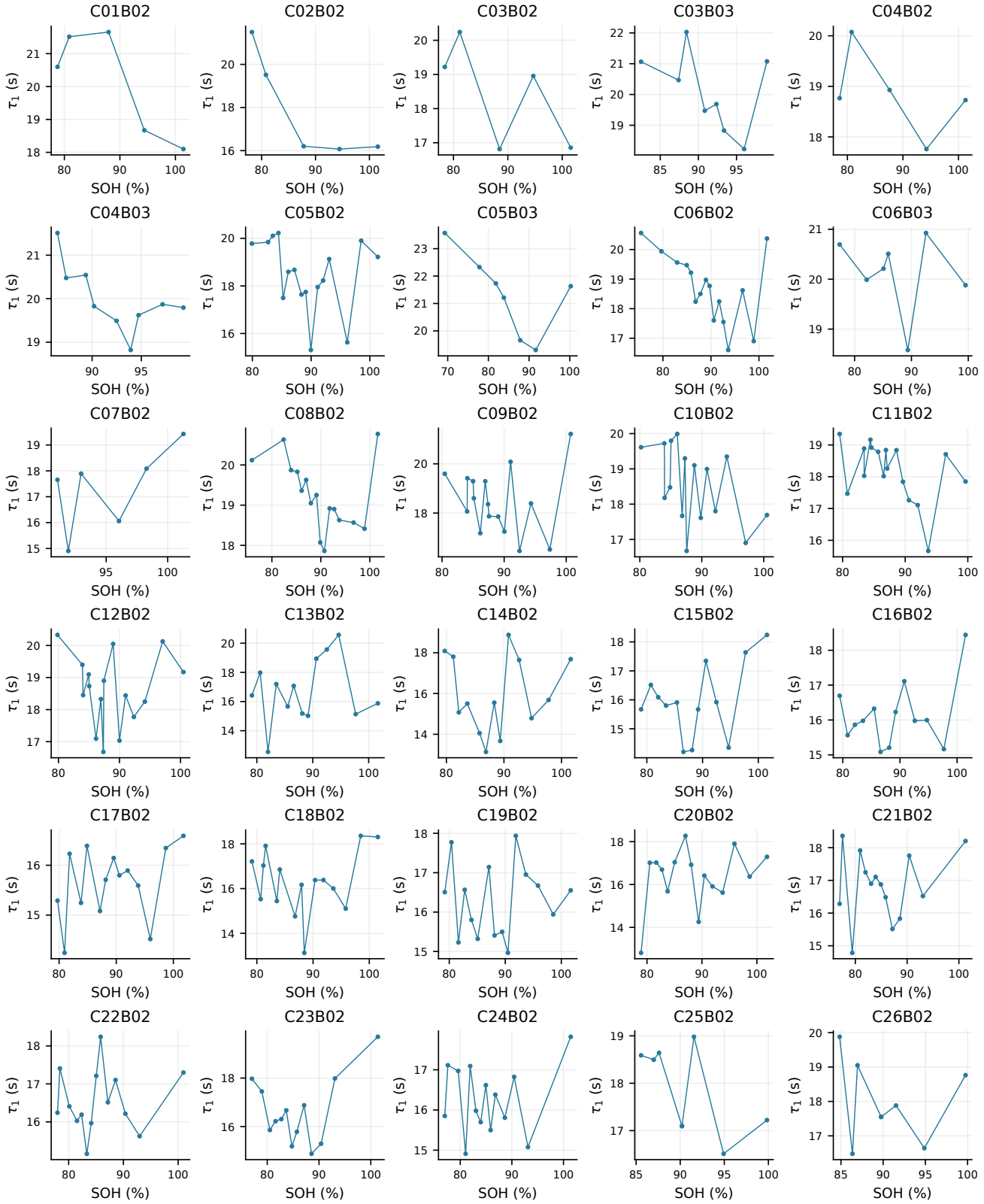


Figure S5: Checkup-median τ_1 versus SOH for all 30 cells. Lines join observations; the full C/B cell identifiers are shown. The operating points are not matched in instantaneous SOC or temperature. These are descriptive trajectories, not causal aging estimates.

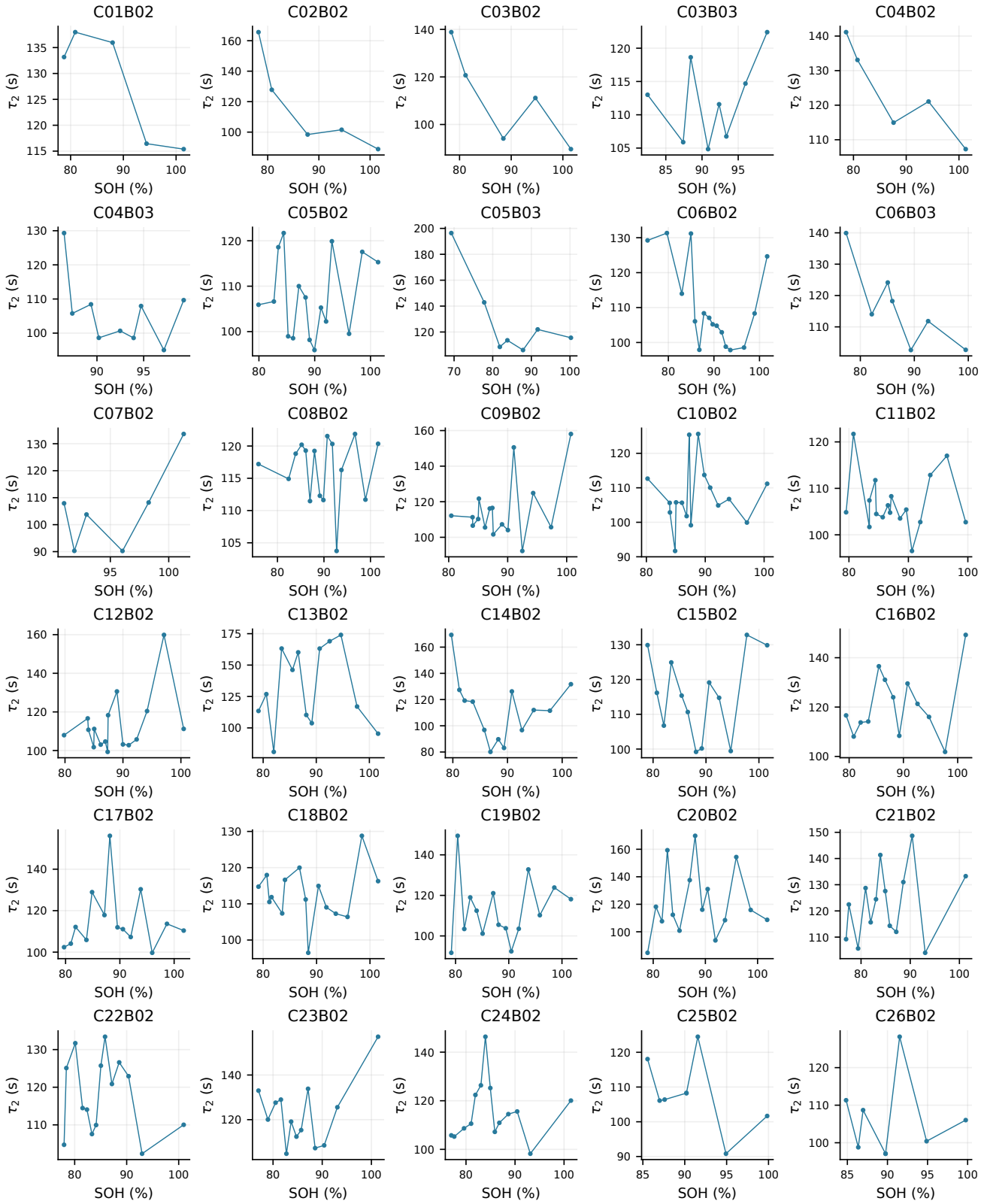


Figure S6: Checkup-median τ_2 versus SOH for all 30 cells. Lines join observations; the full C/B cell identifiers are shown. The operating points are not matched in instantaneous SOC or temperature. These are descriptive trajectories, not causal aging estimates.

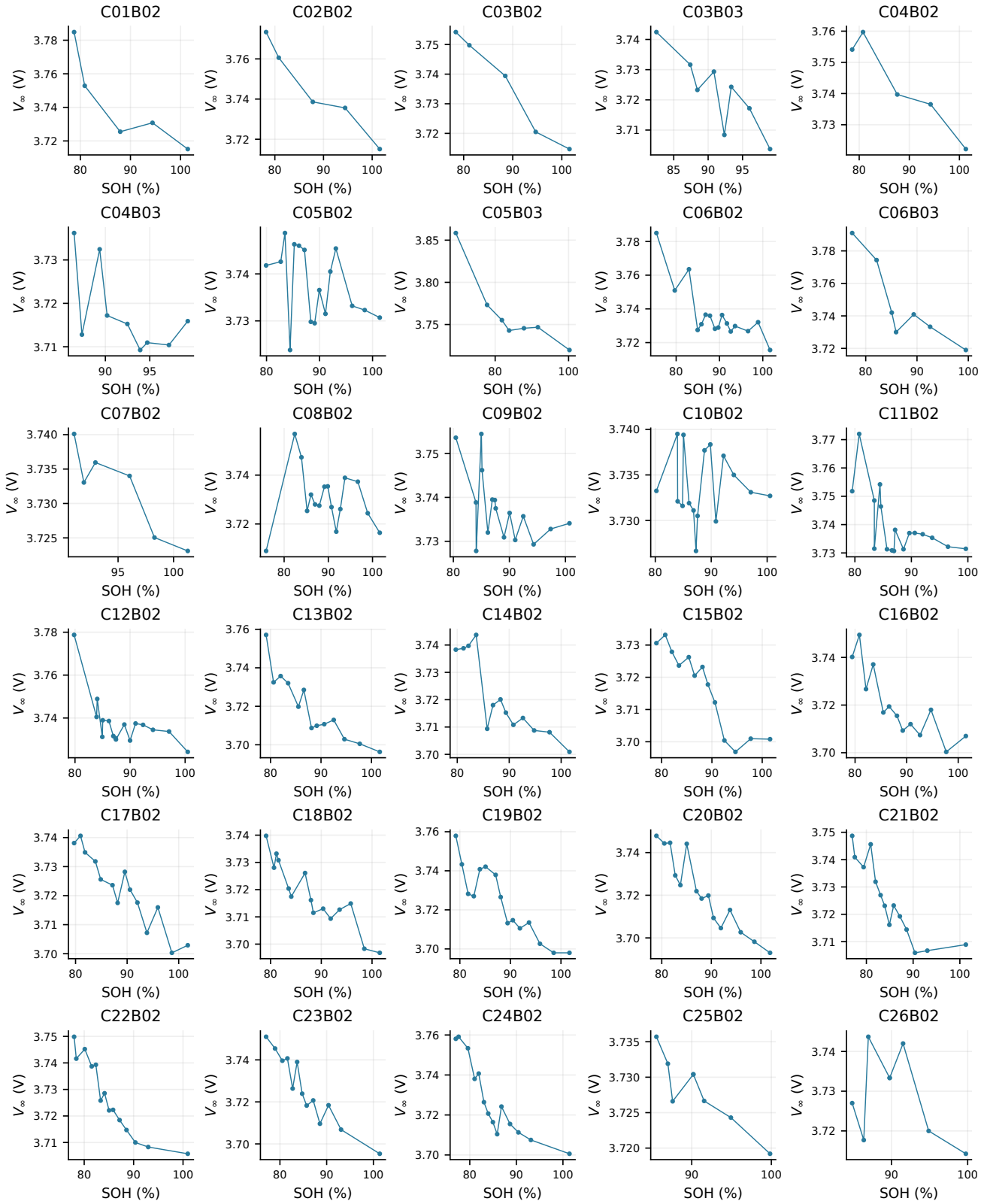


Figure S7: Checkup-median V_∞ versus SOH for all 30 cells. Lines join observations; the full C/B cell identifiers are shown. The operating points are not matched in instantaneous SOC or temperature. These are descriptive trajectories, not causal aging estimates.

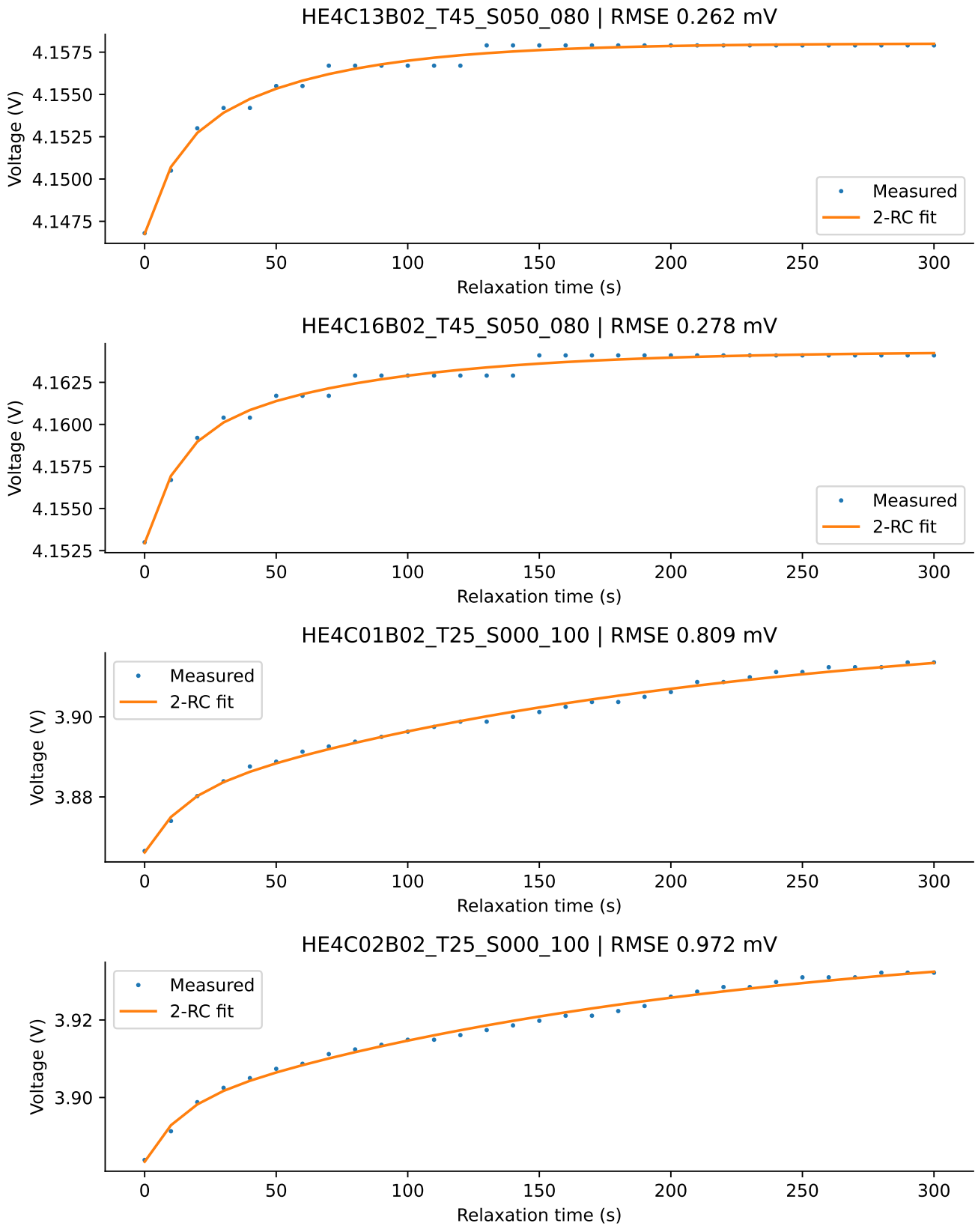


Figure S8: Representative two-exponential fits spanning low and high residual RMSE within the 353-segment diagnostic sample. The larger-residual examples remain sub-millivolt fits; the larger residuals indicate poorer agreement relative to this dataset, rather than failed optimization.

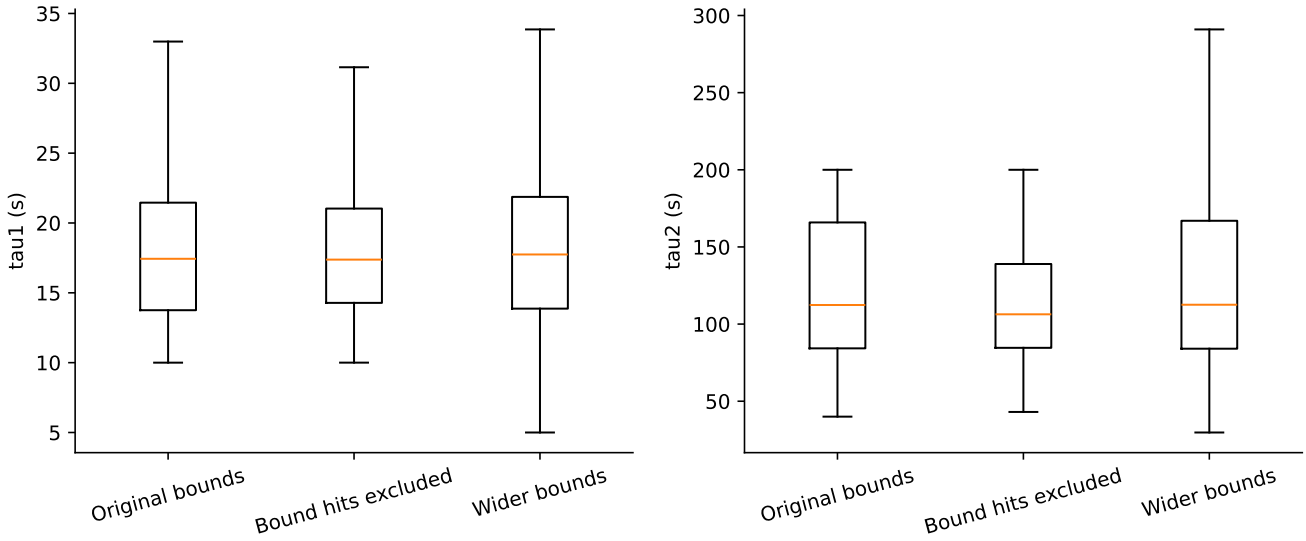


Figure S9: Time-constant distributions under the default and wider bounds and after excluding bound-reaching measurements. T1 and T2 denote τ_1 and τ_2. Population changes and shifts under wider bounds must be distinguished.

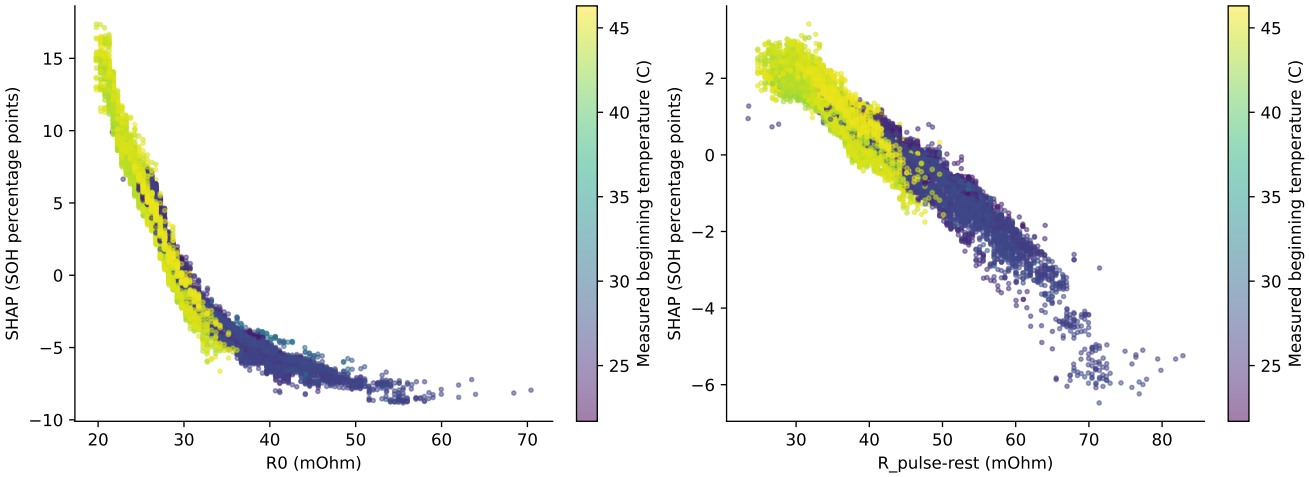


Figure S10: Exploratory held-out XGBoost resistance–temperature dependence. The resistance axes correspond to R_0 and R_{pr}. SHAP values are in SOH percentage points; colors show the measured beginning temperature. These associations do not identify causal temperature effects.

Table S15: Descriptive within-cell correlations between checkup-median features and SOH.

Feature	$\rho < 0$ cells	Median ρ	Minimum ρ	Maximum ρ
R_0	30/30	-0.999	-1.000	-0.943
R_1	30/30	-0.816	-1.000	-0.086
R_2	29/30	-0.643	-1.000	0.205
R_{pr}	30/30	-1.000	-1.000	-0.943
τ_1	20/30	-0.207	-0.900	0.714
τ_2	15/30	-0.012	-0.900	0.486
V_∞	30/30	-0.889	-1.000	-0.053

Each cell contributes one coefficient, calculated from 5–17 checkup-level pairs (median 13). Ties were assigned average ranks. For R_{pr}, 18 cells have $\rho = -1$; the median remains -1.000 when R_{pr} is used before six-decimal rounding (with SOH unchanged), or when the five cells with ties in either variable are excluded. A negative correlation indicates an increase as SOH decreases. Measurement SOC and temperature are not matched across checkups; these are descriptive trends, not estimates of a causal aging effect.

Table S16: Incidence of fitted time constants at the default bounds (12,643 primary measurements).

Bound	Count	Percent (%)
$\tau_1 = 10$ s	1102	8.716
$\tau_1 = 40$ s	76	0.601
$\tau_2 = 40$ s	12	0.095
$\tau_2 = 200$ s	2067	16.349
At least one bound	3245	25.666

A value is classified as reaching a bound within 0.001 s. The any-bound row counts measurements once, even if more than one bound is reached.

Table S17: Sensitivity and transfer tests.

Test	Model	Inputs	n	MAPE (%)	RMSE (pp)	R^2
Bound-free	XGBoost	M1	9398	2.1358	2.601	0.8310
Bound-free	XGBoost	M4	9398	1.0754	1.284	0.9588
Quality screen	XGBoost	M1	12596	2.0114	2.461	0.8511
Quality screen	XGBoost	M4	12596	1.0337	1.246	0.9618
Wider bounds	XGBoost	M1	12643	2.0531	2.515	0.8439
Wider bounds	XGBoost	M4	12643	1.0498	1.260	0.9608
Temperature out	XGBoost	M1	12643	7.6768	8.681	-0.8593
Temperature out	XGBoost	M4	12643	6.7007	7.788	-0.4963
SOC window out	XGBoost	M1	12643	2.6111	2.946	0.7859
SOC window out	XGBoost	M4	12643	2.6976	2.833	0.8020
CC to dynamic	XGBoost	M4	644	3.1904	3.413	0.4406
CC to dynamic	GPR	M4	644	4.6805	5.829	-0.6318
CC to dynamic	Ridge	M4	644	3.5432	4.170	0.1648

Bound-free and quality-screen results use smaller populations. Their pooled errors should not be interpreted as matched estimates of improvement over the primary analysis. Paired comparisons on common held-out measurement IDs are in Table S6.

Table S18: Recorded desktop timing for M4 (median across the five outer folds).

Model	Fit and selection (s)	Single query (ms)	Batch per row (ms)
XGBoost	222.015	0.477	0.0063
GPR	8.406	0.547	0.4139
Ridge	0.422	0.216	Below timer resolution

Fit timings include the implemented model-selection step. XGBoost uses 50 nested-search trials, GPR uses one bounded kernel optimization on a training subset, and Ridge uses an alpha grid; their search budgets differ. Query timings exclude acquisition and ECM extraction. These are desktop timings under the recorded workload, not embedded BMS benchmarks.

Table S19: XGBoost held-out interventional TreeSHAP magnitudes and within-model shares.

Feature	M1	M2	M3	M4
R_0	3.990 / 42.73	3.922 / 29.59	4.822 / 38.85	4.331 / 31.08
R_1	0.493 / 5.28	0.403 / 3.04	0.493 / 3.97	0.328 / 2.35
R_2	0.775 / 8.30	0.272 / 2.05	1.081 / 8.71	0.098 / 0.70
R_{pr}	1.683 / 18.02	1.443 / 10.89	1.982 / 15.97	1.089 / 7.82
τ_1	0.407 / 4.36	0.238 / 1.80	0.518 / 4.17	0.284 / 2.04
τ_2	0.621 / 6.65	0.148 / 1.12	0.870 / 7.01	0.076 / 0.55
V_∞	1.368 / 14.65	1.554 / 11.73	1.666 / 13.42	1.571 / 11.27
T_{age}	–	0.854 / 6.45	–	1.005 / 7.21
T_{beg}	–	2.167 / 16.36	–	2.093 / 15.02
T_{end}	–	2.249 / 16.97	–	1.983 / 14.23
s_{min}	–	–	0.436 / 3.51	0.530 / 3.80
s_{max}	–	–	0.545 / 4.39	0.545 / 3.91

Each entry is mean absolute SHAP in SOH percentage points / within-model share in percent. Shares have a different denominator for each model. A cell-balanced background of 32 training rows is used per fold. The original path-dependent M1 and M4 explanations are separately retained in Table S11.

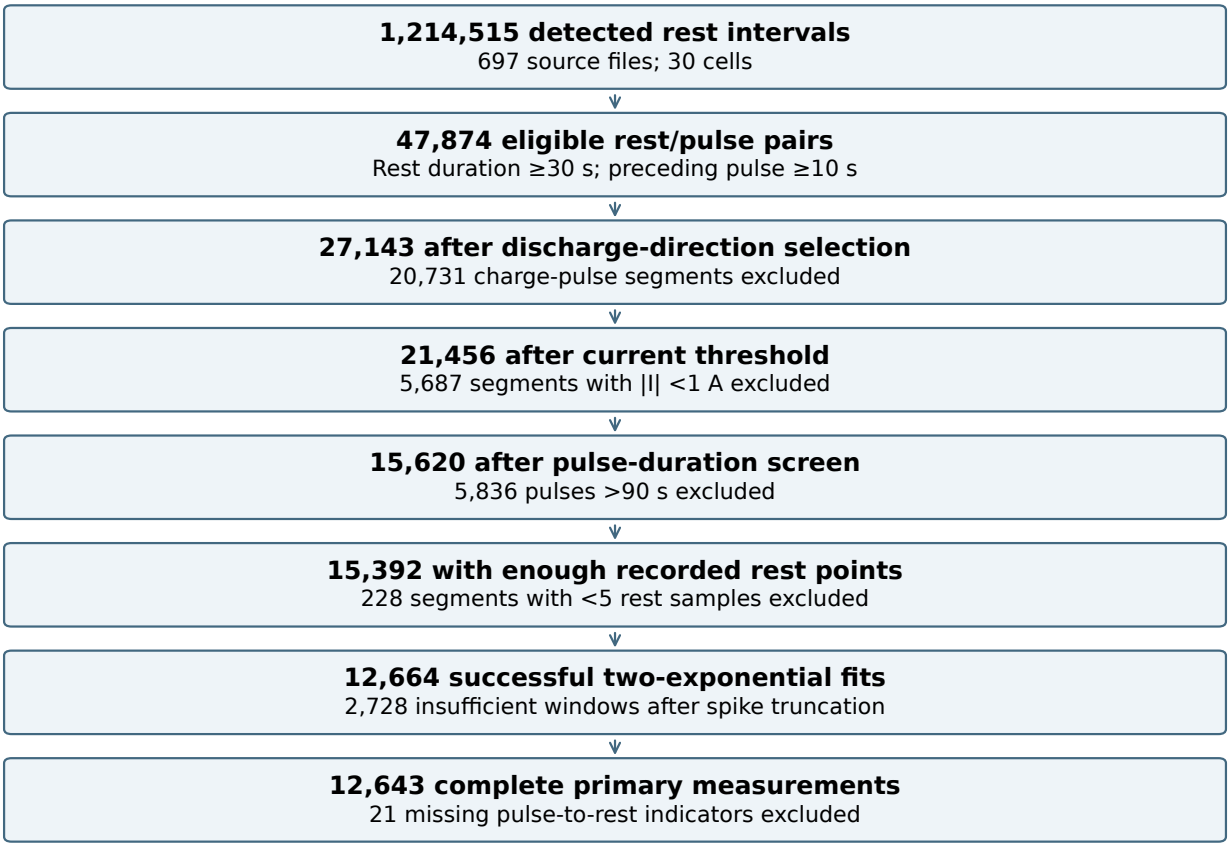


Figure S11: Measurement flow. Counts represent intervals or segments, not independent cells. Of 2933 spike-truncation events, 205 retain enough points and 2728 contribute to the insufficient-window exclusion.

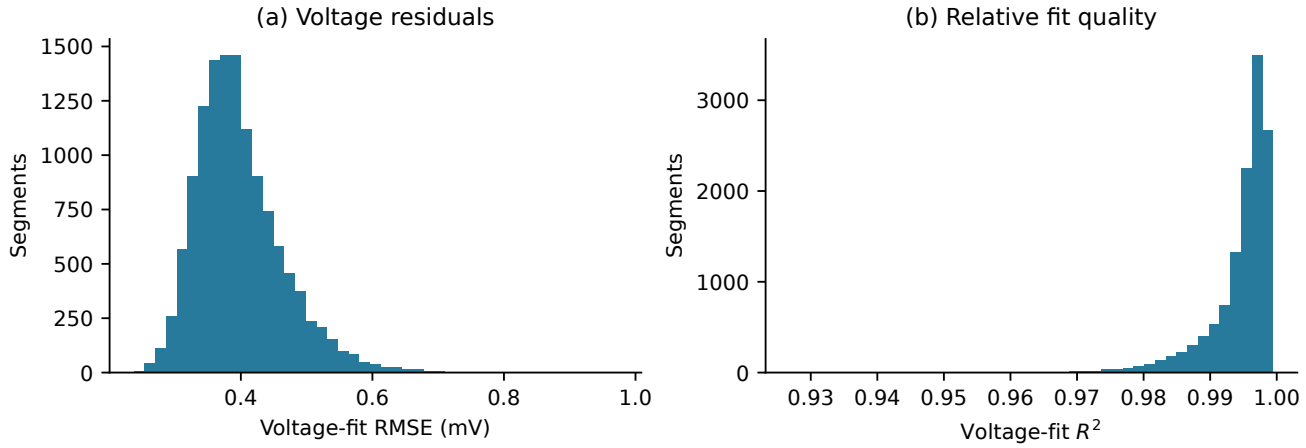


Figure S12: Fit-quality distributions for the primary population. A small voltage residual does not establish precise component parameters.

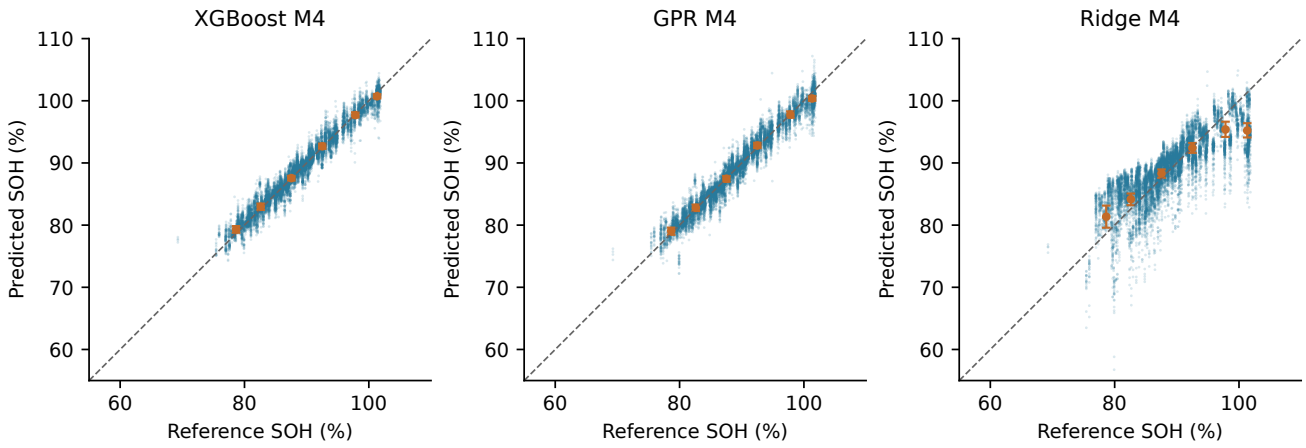


Figure S13: M4 held-out predictions for all three learners. Individual measurements and binned means are shown. Cell-bootstrap 95% intervals concern binned mean predictions, not individual predictions.

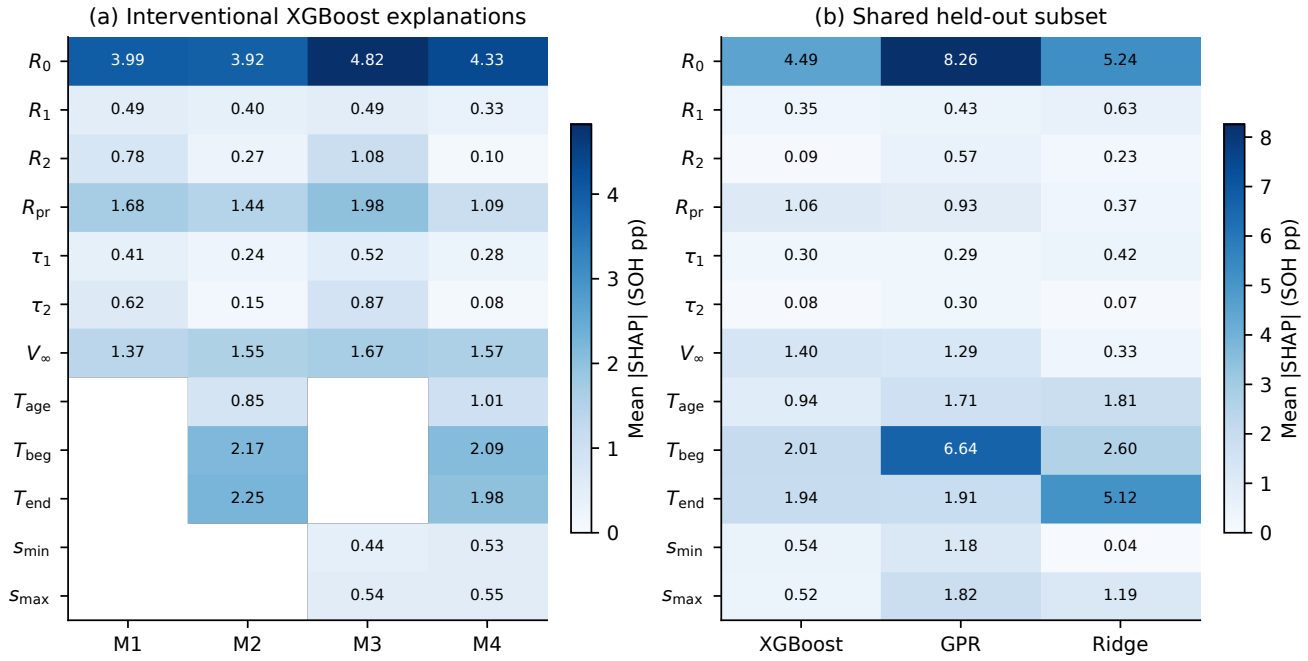


Figure S14: Additional interventional absolute attributions in SOH percentage points: (a) all held-out XGBoost rows; (b) the same 150 held-out rows across algorithms. These explanations differ from the path-dependent values reported in main Figures 9–10 and 13–15 and Table S11. GPR uses approximate KernelSHAP.

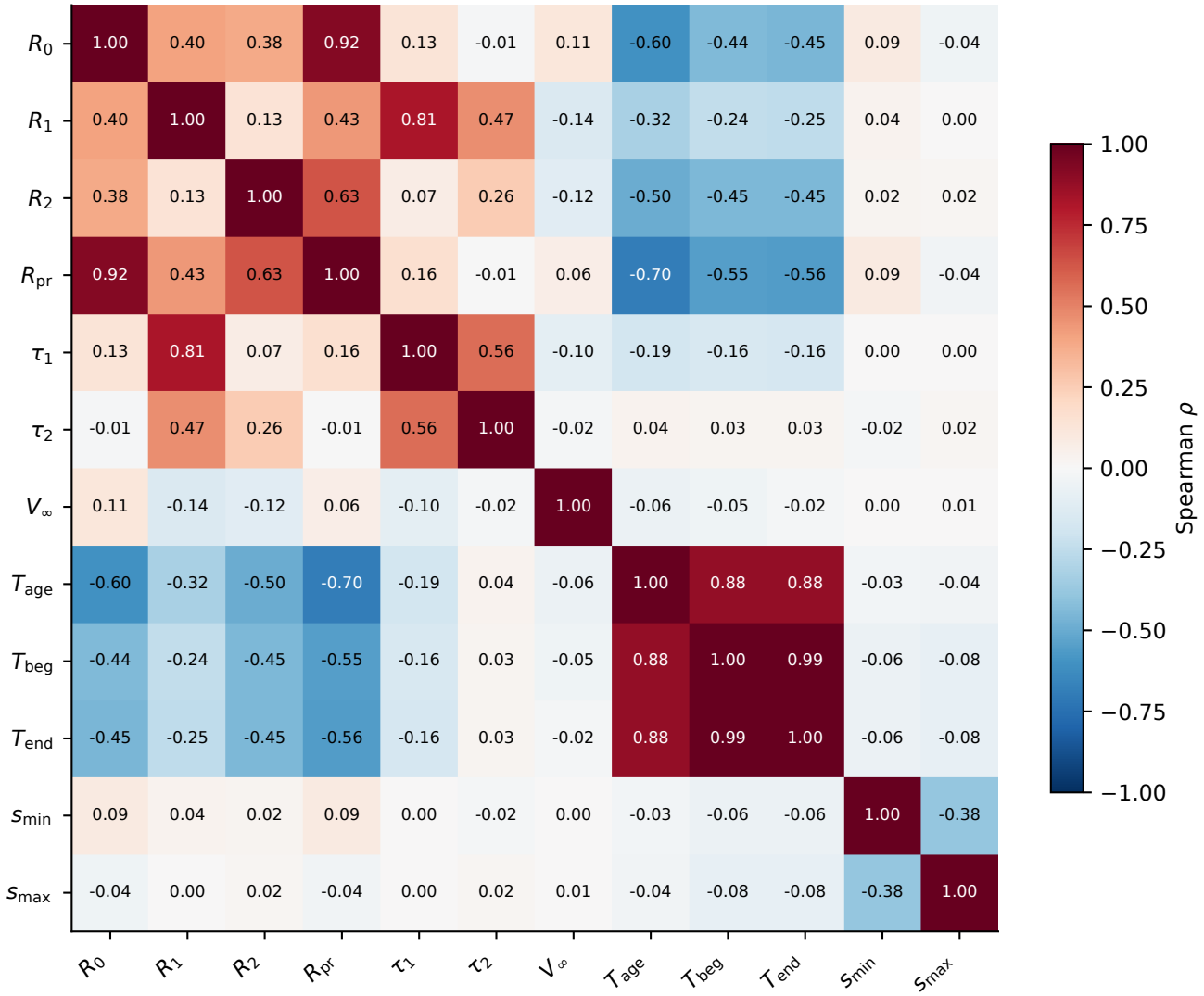


Figure S15: Spearman input correlations in the primary population. This pooled descriptive matrix does not account for within-cell dependence and is not a significance test.

S1 Software Environment and Reproducibility

S1.1 Computational environment

The analysis environment recorded in the execution log comprised Python 3.12.10, NumPy 2.5.2, pandas 3.0.5, SciPy 1.16.3, scikit-learn 1.9.0, XGBoost 3.4.1, SHAP 0.52.0, Optuna 4.9.0, and Matplotlib 3.11.1. Parameter fitting used SciPy's `curve_fit` with the Trust Region Reflective method.

Computations were performed on an AMD Ryzen 7 9700X computer with 64 GB RAM. Extraction used four workers; non-GPR outer-fold work used up to five concurrent workers with one numerical-library thread per fit. GPR folds ran sequentially with eight numerical-library threads. Timings reflect this computer and its concurrent workload; they are not measurements of embedded-BMS latency. The dependency versions and analysis settings are supplied in `config/analysis_settings.json` and `requirements.txt` in Supplementary Software S1.

S1.2 Input definitions, precision, and model-selection settings

Code columns `R_DCIR`, `T1`, `T2`, and `OCV` correspond to R_{pr}, τ_1, τ_2, and V_∞; the supplementary notation T_{age} is identical to T_{cha}.

The common primary matrix contains 12,643 measurements from 30 cells. Exported resistances use six decimal places, time constants and V_∞ four, temperatures one, and SOC-window fractions four. The target is the reference-discharge capacity rounded to 0.001 Ah, divided by 2.5 Ah and rounded to four decimal places. Python's scalar rounding convention is retained. Identifiers, capacity, checkup number, and file order are not model features.

XGBoost hyperparameters were selected by 50 Optuna trials and five cell-disjoint inner folds within each outer training set, minimizing mean inner-fold RMSE. The search covered `n_estimators` from 100 to 1500 in steps of 50, `max_depth` from 2 to 10, and `learning_rate` from 0.005 to 0.3 on a logarithmic scale. Both `subsample` and `colsample_bytree` ranged from 0.5 to 1.0; `reg_lambda` ranged from 0.1 to 10 on a logarithmic scale. Trials ran sequentially. The base seed was 2026; outer-fold models and the corresponding Optuna samplers used seeds 2026–2030. Inner-fold model seeds incremented from the corresponding outer-fold seed. The selected M1–M4 settings are tabulated in Table S5. GPR and Ridge settings are summarized in Table S10; the complete machine-readable record covers 204 outer fits across 44 scenarios in `config/model_settings.json`. The fixed outer cells are listed in Table S1 and `config/fold_assignments.csv`.

All primary models use identical rounded inputs, SOH labels, and outer test cells. Bound exclusion, fit-quality screening, wider bounds, feature removal, and held-out-condition/protocol evaluations remain separate sensitivity analyses. The corresponding populations and split conventions are listed in `config/scenarios.json`. The GPR final fit conditions on all outer-training rows; the 1500-row limit applies only to kernel tuning.

S1.3 Code package and explicit analysis calls

Supplementary Software S1 contains one Python source file, `battery_analysis.py`, with English documentation. Its functions cover reading raw measurements, relaxation detection, equivalent-circuit feature extraction, model fitting, cell-disjoint validation, feature attribution, and sensitivity calculations. Importing or directly opening the module does not start an analysis. Functions are called explicitly and return in-memory objects; saving a table or creating and saving a figure is a separate action chosen by the user. The README provides usage examples and describes the supplied reference files. ChatGPT/Codex (OpenAI; GPT-5.6 Sol and GPT-6 Astra) assisted with preparing and editing the analysis code. Parameter fitting, model training, predictions, and numerical summaries were computed by the Python workflow described above.

The processed primary matrix is supplied in `data/processed_features.csv`, and the full-precision fit diagnostics in `data/extracted_features.csv`. Configuration files record the folds, selected settings, and seeds. The `reference` directory contains stored numerical results, including held-out predictions and pooled metrics, for optional comparisons. The `verify_predictions` function recomputes error metrics from a supplied prediction table and returns its comparison with supplied reference values.

Raw voltage, current, time, and temperature measurements are obtained separately from the original dataset at `https://doi.org/10.14279/depositonce-17598`. The raw-data directory is passed by the user; no personal directory is embedded in the shared module. The package does not duplicate the raw archive. The figure-data records document the coordinates and original point order used for Figures 4–6 and the SHAP values used for Figure 15; cell-level summaries support Figure S16 and Table S20.

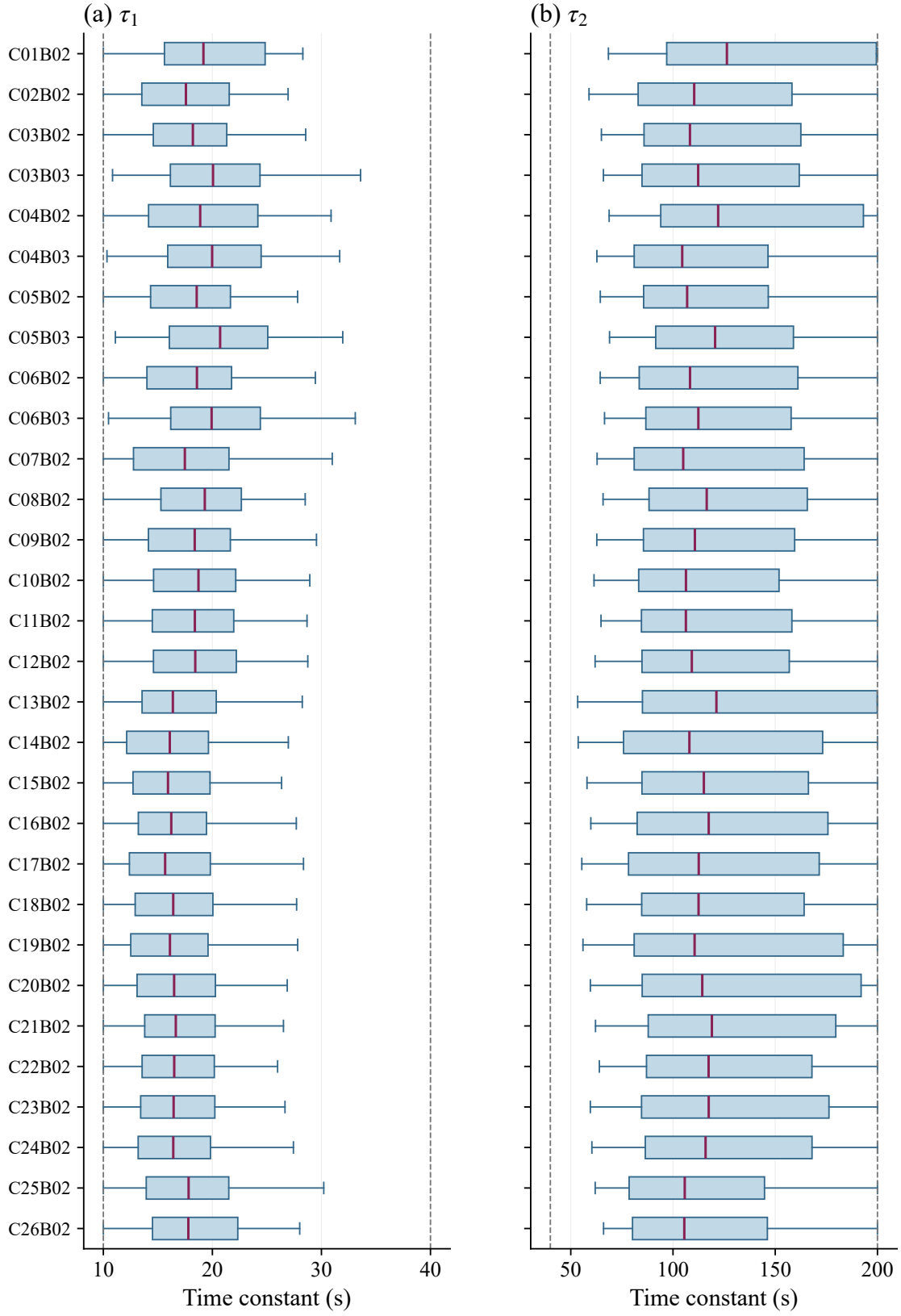


Figure S16: Cell-specific distributions of τ_1 and τ_2 for all 12,643 primary measurements from 30 cells. Boxes span the interquartile range and red lines mark medians; whiskers extend to the most extreme observations within the 5th–95th percentile range. Observations beyond the whiskers are omitted from this display but remain in the analysis. Dashed vertical lines mark the fitting bounds. Each distribution pools that cell's checkups and operating points and is descriptive, not a matched-condition aging comparison.

Table S20: Cell-specific fitting-bound incidence in the unchanged primary population. Entries are count (% within cell); n is the number of measurements, not independent cells.

Cell	n	τ_1: 10 s	τ_1: 40 s	τ_2: 40 s	τ_2: 200 s	Any bound
C01B02	158	11 (7.0)	0 (0.0)	0 (0.0)	37 (23.4)	48 (30.4)
C02B02	154	18 (11.7)	0 (0.0)	0 (0.0)	27 (17.5)	45 (29.2)
C03B02	154	9 (5.8)	1 (0.6)	0 (0.0)	23 (14.9)	33 (21.4)
C03B03	309	12 (3.9)	6 (1.9)	0 (0.0)	39 (12.6)	57 (18.4)
C04B02	152	12 (7.9)	2 (1.3)	0 (0.0)	33 (21.7)	46 (30.3)
C04B03	353	15 (4.2)	3 (0.8)	0 (0.0)	37 (10.5)	55 (15.6)
C05B02	536	48 (9.0)	6 (1.1)	0 (0.0)	73 (13.6)	127 (23.7)
C05B03	218	9 (4.1)	2 (0.9)	0 (0.0)	28 (12.8)	39 (17.9)
C06B02	532	42 (7.9)	3 (0.6)	0 (0.0)	80 (15.0)	124 (23.3)
C06B03	236	9 (3.8)	2 (0.8)	0 (0.0)	24 (10.2)	35 (14.8)
C07B02	203	21 (10.3)	5 (2.5)	0 (0.0)	37 (18.2)	62 (30.5)
C08B02	528	44 (8.3)	4 (0.8)	0 (0.0)	75 (14.2)	122 (23.1)
C09B02	565	64 (11.3)	6 (1.1)	0 (0.0)	71 (12.6)	140 (24.8)
C10B02	575	53 (9.2)	3 (0.5)	0 (0.0)	75 (13.0)	131 (22.8)
C11B02	596	58 (9.7)	3 (0.5)	0 (0.0)	84 (14.1)	144 (24.2)
C12B02	566	46 (8.1)	5 (0.9)	0 (0.0)	82 (14.5)	133 (23.5)
C13B02	488	39 (8.0)	1 (0.2)	4 (0.8)	111 (22.7)	154 (31.6)
C14B02	479	61 (12.7)	1 (0.2)	3 (0.6)	94 (19.6)	158 (33.0)
C15B02	494	57 (11.5)	1 (0.2)	3 (0.6)	95 (19.2)	155 (31.4)
C16B02	485	30 (6.2)	0 (0.0)	1 (0.2)	89 (18.4)	120 (24.7)
C17B02	525	53 (10.1)	2 (0.4)	0 (0.0)	89 (17.0)	144 (27.4)
C18B02	559	51 (9.1)	1 (0.2)	0 (0.0)	96 (17.2)	148 (26.5)
C19B02	560	62 (11.1)	3 (0.5)	0 (0.0)	109 (19.5)	174 (31.1)
C20B02	563	53 (9.4)	1 (0.2)	0 (0.0)	116 (20.6)	169 (30.0)
C21B02	516	48 (9.3)	1 (0.2)	0 (0.0)	104 (20.2)	153 (29.7)
C22B02	510	46 (9.0)	1 (0.2)	0 (0.0)	95 (18.6)	141 (27.6)
C23B02	477	45 (9.4)	0 (0.0)	0 (0.0)	88 (18.4)	133 (27.9)
C24B02	508	37 (7.3)	1 (0.2)	1 (0.2)	84 (16.5)	123 (24.2)
C25B02	326	28 (8.6)	5 (1.5)	0 (0.0)	34 (10.4)	67 (20.6)
C26B02	318	21 (6.6)	7 (2.2)	0 (0.0)	38 (11.9)	65 (20.4)